UNIVERSITY OF TARTU
Faculty of Science and Technology
Institute of Technology

Aleksandra Panfilova

Optimization of Sic1-Cln2-based phosphodegron tag for inducible protein degradation

Master's Thesis (30 ECTS)

Curriculum Bioengineering

Supervisor(s):
Research Fellow, PhD Nastassia Shtaida
Professor, PhD Mart Loog

Tartu 2021

Optimization of Sic1-Cln2-based phosphodegron tag for inducible protein degradation

Abstract:

Precise regulation of protein abundance in the cell would be instrumental in both research and industry. A variety of tools exists for the regulation of protein expression at the transcriptional level. However, there is a shortage of tools that would allow control over already expressed proteins. In this study, we exploit the native cell cycle regulation system of *Saccharomyces cerevisiae* to develop a system for targeted inducible protein degradation. Using sequence elements that modulate cyclin-dependent kinase (CDK) substrate specificity, we generated a set of phosphodegron tags that have diverse effects on degradation rates of the tagged proteins. The control over the system is provided by conditional expression of the stabilized version of cyclin Clb3, which drives CDK-dependent phosphorylation of the tag, and F-box protein Grr1, which recognizes phosphorylated tag and label it for further degradation. In the course of this work, we have designed a set of phosphodegron tags that can be used for the regulation of the protein abundance in the cell and its maintenance at desirable levels that can be useful for the industrial production of value-added products. In addition, we discovered that Cks1 priming effect on the multisite phosphorylation is not only distance-, but, likely, also context-dependent which might be of interest for fundamental research.

Keywords: Cell cycle, degrons, cyclins, Sic1

CERCS: P310 Proteins, enzymology; SPECIFICATION: Protein kinase signaling networks in eukaryotic cell cycle.

Sic1-Cln2-põhise fosfodegroni märgise optimeerimine indutseeritava valgu lagundamiseks

Lühikokkuvõte:

Rakusiseste valkude arvukuse täpne reguleerimine on oluline nii teadustöös kui ka tööstuses. Valgu ekspressiooni reguleerimiseks transkriptsiooni tasandil eksisteerib mitmesuguseid meetodeid. Kuid on puudus meetoditest, mis võimaldaksid kontrollida juba ekspresseeritud valkude tasemeid. Selles uuringus kasutame *Saccharomyces cerevisiae* rakutsükli reguleerimissüsteemi, et tekitada moodus indutseeritava valgu lagundamiseks. Kasutades

tsükliinisõltuva kinaasi (CDK) substraadi spetsiifilisust moduleerivaid järjestuselemente, lõime fosfodegroni märgiste komplekti, mis muudavad valkude lagunemiskiirusi. Kontrolli süsteemi üle tagab tsükliini Clb3 stabiliseeritud versiooni tinglik ekspresseerimine, mis juhib märgise CDK sõltuvat fosforüülimist, ja F-box-valk Grr1, mis tunneb ära fosforüülitud märgise ja märgistab selle edasiseks lagundamiseks. Selle töö käigus oleme välja töötanud fosfodegroni märgiste komplekti, mida saab kasutada raku valkude arvukuse reguleerimiseks ja selle säilitamiseks soovitud tasemel, mis võib olla kasulik lisandväärtus toodete tööstuslikuks tootmiseks. Lisaks avastasime, et Cks1 stimuleerib mitme saidi fosforüülimist ja see ei ole mitte ainult järjestusest sõltuv, vaid tõenäoliselt ka kontekstist sõltuv, mis pakub fundamentaaluuringute jaoks huvi.

Võtmesõnad: Rakutsükkel, degronid, tsükliinid, Sic1

CERCS: P310 Proteiinid, ensümoloogia; TÄPSUSTUS: Proteiini kinaasid rakutsükli regulaa-toritena.

TABLE OF CONTENTS

TERMS, ABBREVIATIONS AND NOTATIONS

3xHA tag (YPYDVPDYA-YPYDVPDYA-YPYDVPDYA) – an HA-epitope tag repeated thrice; HA tag is a 98-106 aa region of a human influenza HemAgglutinin.

Cdc28 is a single central CDK of *S. cerevisiae*.

CDK is an abbreviation from cyclin-dependent kinases, a family of serine/threonine protein kinases playing a key role in cell cycle regulation.

Cks1 is a small polypeptide that binds to a larger lobe of the Cdc28 and promotes multisite phosphorylation by binding downstream phosphosites after priming site phosphorylation.

Cln2 is a *S. cerevisiae* G1/S cyclin, contributing to Sic1 degradation and localized mostly in the cytoplasm.

Cyclins are a family of proteins with a common feature of binding and activating CDKs. They do not possess any enzymatic activities by themselves. Still, they contain binding regions for different CDK's substrates and localization sequences, which define substrate specificity and subcellular locations of the CDK-cyclin complex.

Degron is a region in a protein sequence important for the regulation of protein degradation. **Phosphodegron** is a degron, which starts to contribute to the degradation of the protein only after being phosphorylated. **Phosphodegron tag** – sequence, which encodes for the phosphodegron itself and elements required for the regulation of phosphorylation, e. g. Cks1 binding sites and docking motifs.

FL phosphodegron tag, or **FL tag,** or **FL** is abbreviation from Full-Length phosphodegron tag, an unmodified Sic1, Cln2-based phosphodegron tag previously designed and tested in in our lab.

Grr1 is an F-box protein that plays a role as a substrate-recognition subunit of SCF ubiquitin-protein ligase (responsible for the binding of target protein).

GSA (GSAGSAAGSGEF) – a flexible protein linker.

NES (NELALKLAGLDINK) – nuclear export signal, DNA region coding for short peptide sequence targeting protein for transportation from nucleus to cytosol.

pADH1 is a sequence located 716 bp upstream of *ADH1* gene start codon and referred to as *ADH1* promoter.

pEstr – synthetic promoter that contains four LexA-binding sites and, in our case, is regulated by **LexA-ER-B112** transcription factor (Ottoz et al., 2014).

pGAL1 – sequence located 453 bp upstream of *GAL1* gene start codon and referred to as *GAL1* promoter.

POI is abbreviature from Protein Of Interest. It is the protein which is a subject of the study or project.

Sic1 is a Cdc28 inhibitor, which inhibits Cdc28-Clb complexes and controls G1/S phase transition.

INTRODUCTION

Precise regulation of protein concentrations in the cell could allow for tight control over its metabolism or enable rewiring of the cell signaling to control cellular behavior. Transcriptional regulation, widely used in synthetic biology, does not allow for rapid change in the protein concentrations. One of the possible solutions can be found in the cell cycle regulatory network. Cyclin-dependent kinases are the key players of this network. Oscillations in their activity, localization, and substrate specificity are precisely controlled by the cyclin subunit currently bound to the kinase. Combining both transcriptional and post-translational regulations results in rapid cyclin turnover during the cell cycle. Cyclins contain special regions, which, being phosphorylated, become targets for proteolytic machinery and are sent for destruction. These sequences are called phosphodegrons.

Cyclins and other cell-cycle-related proteins can be sources of various regulatory protein domains that, combined and fused to a third protein (reporter protein or metabolic enzyme), might lead to a new outcome in protein behavior.

In this study, we worked on developing and optimizing the cell-cycle-independent, cytoplasmic, inducible, targeted protein degradation system. A set of phosphodegron tag variants were designed on the basis of the Sic1-Cln2-based tag, previously designed in our lab. It consists of the N-terminal part of cyclin-dependent kinase inhibitor Sic1, C-terminal part of *Saccharomyces cerevisiae* cyclin Cln2 (Cln2 degron), PxF docking motif (Clb3 docking motif from Ypr174c protein), and C-terminal part of Sic1 without its inhibitory domain. Endogenous components of the cell cycle regulation system, Clb3 cyclin and Grr1 F-box protein, were put under the tightly controllable promoters to make the system inducible. Clb3 was synthetically modified to localize at the cytoplasm and be stable through the whole cell cycle after the induction. To visualize the effect of phosphodegron tagging on protein stability, mCherry fluorescent protein expressed from constitutive promoter was used as a reporter.

Each tag variant contained a phosphodegron module recognized by Grr1, but other regulatory elements were different from tag to tag. By testing different variants, we wanted to get, first, shortest functional tag performing on the same level as a full-length initial tag, and, second, a set of tags providing different half-lives and downregulation levels for the tagged protein.

1 LITERATURE REVIEW

1.1 Phosphorylation

Introduction to the role of phosphorylation in the cell cycle control system

The cell cycle control system is a regulatory network controlling proteins that execute cell cycle events. The *Saccharomyces cerevisiae* mitotic cell cycle, which is an eukaryotic mitotic cell cycle, is divided into four phases: G1, S, G2, and M. There are three major regulatory transitions, or checkpoints, during the cell cycle, and they are regulated by the cell cycle control system. Depending on whether specific passing criteria are met or not, the cell cycle either continues or is arrested until the defects are repaired, or conditions change. These checkpoints are Start (G1 phase), G2/M (G2 phase), and metaphase-to-anaphase (M phase).

The cell cycle control system must be at the same time robust to ensure the precise temporal order of events and flexible to quickly respond to changes in internal and external conditions. This is enabled by a combination of many signaling pathways, where transcriptional regulation, more rigid and slow, is complemented by post-translational regulation, which allows for rapid changes in protein behavior.

One of the most common types of post-translational modifications in eukaryotes is phosphorylation. As a regulation tool, it is involved in many basic cellular processes, including those tightly connected to the cell cycle. Protein phosphorylation may result in different outcomes: it can affect the enzymatic activity of a protein, its subcellular localization, and affinity to a substrate or ligand. Presence of more than one phosphorylation site in the protein sequence adds complexity and variability to the signaling network. For example, phosphorylation at one site or set of sites can send a protein for degradation (Skowyra et al., 1997), while other sites of the same protein, being phosphorylated, activate or stabilize the protein (Bononi et al., 2011), and that results in different cellular behavior. In addition to that, phosphorylation is a reversible modification.

This variability in the resulting phosphorylation pattern allows for multi-input-multi-output signaling, which is crucial for the regulation of a process as complex as the cell cycle. In addition to that, protein kinases catalyzing phosphorylation reactions can be inhibited or activated, and their substrate specificity is, in some cases, also a subject for regulation (Jordan et al., 2000; Morgan, 2007).

Protein kinases and phosphorylation reaction

Protein kinases are enzymes that catalyze a transfer of one or multiple phosphoryl groups (PO_3^{2-}) from an ATP molecule to a specific amino acid in a substrate protein. The main kinases responsible for the cell cycle regulation are serine/threonine kinases, which phosphorylate OH group of either Ser or Thr residues of a protein molecule by exchanging H^+ from the OH group to the PO_3^{2-}. Protein kinases have a bi-lobate tertiary structure, with a smaller lobe from the N-terminus and a larger one from the C-terminus. The ATP molecule used as a phosphate group donor is located in the cleft between two lobes, an active site of protein kinases (Morgan, 2007). Since ATP molecules in living cells are usually bound to the Mg^{2+} ions, there is a complex of ATP with Mg^{2+} inside an active site of protein kinases. By hydrogen and Mg^{2+} ion bonding with several amino-acid residues, an ATP molecule is held in a position oriented toward the exit of a cleft, near which a substrate binds a larger lobe. One of the amino acids in the activation loop facilitates the transfer of the phosphoryl group from ATP to the target phosphorylation site (phosphosite). The residue of this amino acid causes partial deprotonation of the OH group and subsequent nucleophilic attack by oxygen in the phosphoryl group (De Bondt et al., 1993; Smith et al., 2011). As mentioned above, protein phosphorylation is reversible. Enzymes that can remove phosphate groups from the site are called protein phosphatases. This reaction is catalyzed by exchanging PO_3^{2-} to H^+ from water, bringing the amino acid to its initial state. For many kinase substrates, there is a phosphatase that would dephosphorylate it. Balance between opposing kinases and phosphatases is one of the tools to control state of the protein (Morgan, 2007).

1.2 Cdc28, the main cyclin-dependent kinase in *S. cerevisiae*

Cdc28, *S. cerevisiae* central CDK

The most important components involved in the cell cycle progression are cyclin-dependent kinases (CDKs), a family of serine/threonine protein kinases. By definition, all CDKs require association with a regulatory cyclin subunit for their enzymatic activation.

In different organisms, the number, size, and structure of CDKs may vary. In *S. cerevisiae*, a common model organism to study the cell cycle, the single central CDK is Cdc28, encoded by *CDC28* gene. The Cdc28 protein (homolog of human Cdk1; Cdc28 is often called Cdk1 in yeast too) is 34 kDa and contains 298 amino acids (Saccharomyces Genome Database, https://www.yeastgenome.org). Similar to other CDKs, Cdc28 needs to be associated with a cyclin subunit for activation (Morgan, 2007).

Cyclins, CDK-activating partners

Cyclins are a family of proteins with a common feature of binding and activating CDKs by inducing conformational changes in the kinase. They do not possess any enzymatic activities but contain binding regions for CDK's substrates and localization sequences, which define substrate specificity and subcellular location of the CDK-cyclin complex. Cyclins are characterized by the cell cycle phases or transition points at which their complexes with Cdc28 are more abundant and active. Generally, they are grouped as G1, G1/S, S, and G2/M cyclins. CDK-G1 cyclin complexes mainly control response to the extracellular factors in the context of the cell cycle, and CDK complexes with other three types of cyclins control cell cycle events: G1/S-cyclins – Start checkpoint, S-cyclins – DNA replication and other S-phase events, and G2/M-cyclins – G2/M transition (Morgan, 2007).

For activation, Cdc28 requires an association with a cyclin subunit because cyclin binding induces several essential structural modifications in Cdc28. Without cyclin, a flexible loop in a larger lobe of Cdc28, known as the activation loop or T-loop, blocks substrate access to ATP and prevents substrate binding. In addition to that, amino acids in the Cdc28 active site are positioned in a way that ATP is wrongly oriented. After the cyclin binding, T-loop and ATP are brought into positions required for binding and phosphorylation of a substrate (Morgan, 2007).

In *S. cerevisiae*, there are nine cyclins that form complexes with Cdc28: Cln3 is a G1, Cln1 and 2 are G1/S, Clb5 and 6 are S and Clb1, 2, 3, and 4 are G2/M phase cyclins. Polypeptide sequences vary from cyclin to cyclin, except the ~100 amino acid region called a cyclin box. The function of this box is central for all cyclins: binding and activation of CDK. Despite the sequence diversity, cyclins share some common structural features. Part of their tertiary structure is relatively well-conserved: a core of two domains, known as cyclin fold, consisting of five alpha-helixes each. The first domain contains a cyclin box, and the second one repeats the arrangement of the first. Outside of the cyclin fold, both sequence and structure differ from cyclin to a cyclin and contain regulatory and targeting domains specific for a particular cyclin class (Morgan, 2007).

Cdc28 is a single kinase regulator facilitating the whole cell cycle, and its activity must oscillate to allow Cdc28 to perform different tasks in every phase. However, Cdc28 levels are relatively constant throughout the cell cycle and its' protein abundance exceeds cyclins' abundance (Ho et al., 2018). Cyclin levels, in contrast, oscillate during different cell cycle phases, and so do levels of corresponding cyclin-Cdc28 complexes. The enzymatic activities

of cyclin-Cdc28 complexes, however, in some cases do not change in coordinated manner with cyclin levels but exhibit a delay. It is caused by Cdc28 regulation through cyclin-independent activation and inhibition, which creates a time gap between the formation of the complex and its activation (Morgan, 2007).

Cdc28 activation and inhibition

Switching the kinase on and off is the primary basic regulatory mechanism of phosphorylation signaling, and the cell cycle control system is not an exception.

Complete activation of Cdc28 and its proper functioning also requires phosphorylation of a Thr 160 residue in the T-loop. This phosphorylation is catalyzed by Cdk-activating kinase Cak1 and, along with cyclin binding, changes the T-loop orientation that facilitates CDK activation (De Bondt et al., 1993; Morgan, 2007; Russo et al., 1996).

There is also inhibitory phosphorylation for Cdc28. Phosphorylation of Tyr 14 residue of the Cdc28 by Swe1 inactivates the cyclin–Cdk complex. Dephosphorylation by the phosphatase Mih1 leads to reactivation. Both Swe1 and Mih1 are regulated by their primary substrates, Cdc28-M-phase cyclin complexes, and are required for controlling G2/M checkpoint (Morgan, 2007).

In addition, Cdc28 activity is inhibited by CDK inhibitors (CKIs), Far1, and Sic1 proteins. These proteins act by directly binding and inactivating cyclin-Cdc28 complexes. Far1 inhibits G1/S cyclin-Cdc28 in the presence of mating pheromones, causing the cell cycle to freeze and initiates a mating response. Sic1 inhibits S or M cyclin-Cdc28 activity in G1. Sic1 is marked for degradation by phosphorylation by G1/S and S cyclin-Cdc28, which allows the cell cycle to move forward (Morgan, 2007).

Cks1 priming

Many important Cdc28 targets have more than one phosphosite. For example, Sic1 has eight phosphosites involved in its degradation (Figure 1). Phosphorylation of five of them is essential for the recognition of Sic1 by the degradation machinery (Hao et al., 2007). The other three phosphosites, located close to the N-terminus of Sic1, are not essential for the recognition, but in case they are missing, Sic1 is not degraded efficiently *in vivo*. It was shown that these three threonine phosphosites serve the so-called ‘priming’ role. Upon their phosphorylation, the affinity of the Cdc28-cyclin complexes towards the other five phosphosites is increased. Moreover, those five phosphosites are grouped into two distant modules (around 20 amino acids apart from each other), and the first module serves both for Sic1

recognition by degradation machinery and for priming the phosphorylation of the second module (Kõivomägi et al., 2011a). This effect of 'priming' phosphosites was shown not only in Sic1 but also in a broad range of Cdc28 targets (Kõivomägi et al., 2013).

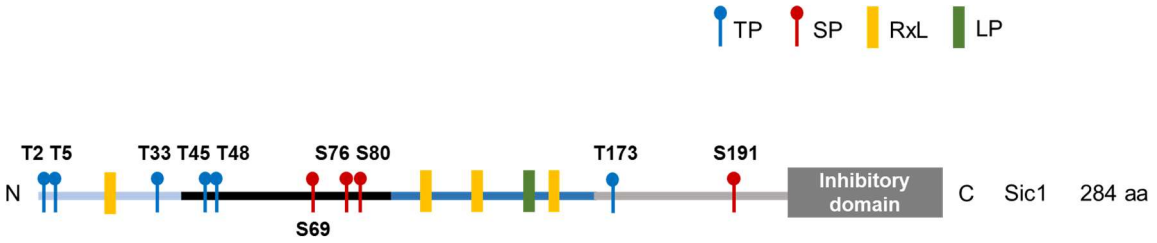

Figure 1. Schematic representation of Sic1, its phosphorylation sites, Clb5- and Cln2-specific docking motifs (RxL and LP, respectively), and inhibitory domain. Five modules of different colors on the scheme represent N-terminal Cks1 docking module (light blue), phosphodegron module (black), cyclin docking module (dark blue), a region containing multisite phosphorylation-terminating phosphosite (light gray), and inhibitory domain (dark gray), respectively. (Figure was adapted from the articles *Cascades of multisite phosphorylation control Sic1 destruction at the onset of S phase,* by Köivomägi et al., 2011 and *A processive phosphorylation circuit with multiple kinase inputs and mutually diversional routes controls G1/S decision*, by Venta et al., 2020).

This 'priming' effect (the increase of Cdc28-cyclin affinity towards targets previously phosphorylated on specific sites) is achieved by the addition of another subunit to the Cdc28-cyclin complex: the Cks1 subunit. Cks1 protein contains a phosphate-binding pocket and binds a larger lobe of a Cdc28 (Figure 2). By simultaneous binding of both Cdc28 and previously phosphorylated site of a substrate, Cks1 increases Cdc28 affinity towards this substrate, therefore promoting downstream multisite phosphorylation of polypeptide chain (McGrath et al., 2013). Cks1 binds only phosphothreonines and not phosphoserines (Kõivomägi et al., 2013).

One of the factors influencing the efficiency of multisite phosphorylation with Cks1 priming is the distance between 'priming' phosphosite and downstream sites. The optimal distance was shown to be 12 amino acids (aa), and up to 16 aa multisite phosphorylation rates were high. All distances below 12 and longer than 20 aa resulted in a rapid decrease of multisite phosphorylation rates (Kõivomägi et al., 2013).

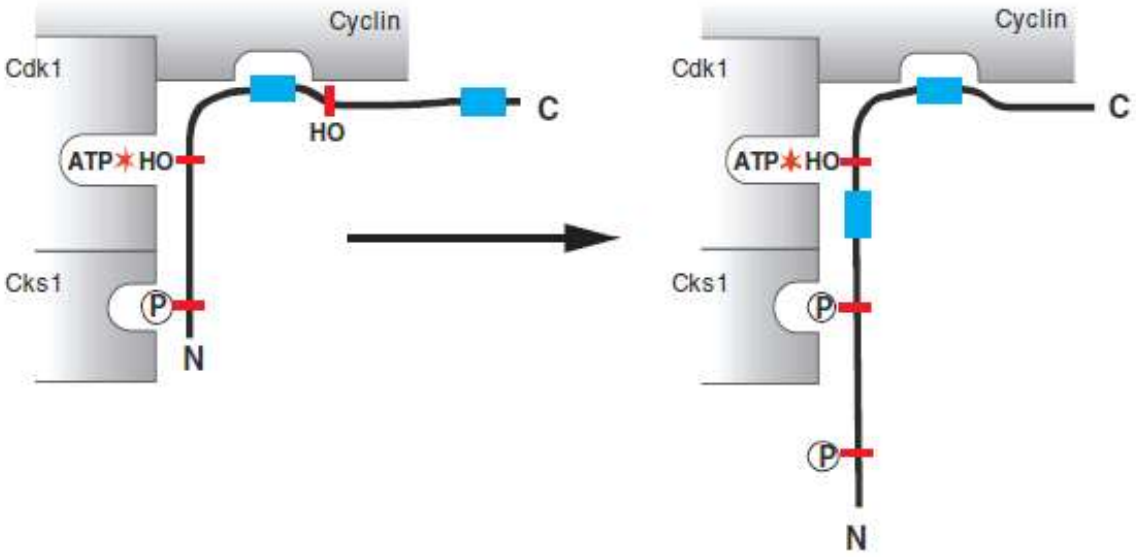

Figure 2. Structure of Cdc28(Cdk1)-cyclin-Cks1 complex. By binding to the phosphorylated site of the substrate, Cks1 increases Cdc28 affinity towards this substrate, therefore, promoting downstream multisite phosphorylation. Blue boxes indicate cyclin docking motifs of the substrate sequence. (Figure was taken from the article *Multistep phosphorylation systems: tunable components of biological signaling circuits,* 2014 by Valk et al.)

As phosphorylation usually has a significant impact on the protein's fate and is especially important for the cell cycle progression, both activity and substrate specificity of Cdc28 are tightly controlled.

1.3 Regulation of Cdc28 target specificity

Cdc28 is a single regulatory kinase that controls cell division. Throughout the cell cycle, it sequentially phosphorylates multiple substrates, and that ensures cell cycle progression and correct ordering. For example, in the late G1/early S-phase, Cdc28-cyclin complexes activate transcription of genes, which code for proteins of the replication machinery. Later in the S phase, the same Cdc28 in the complex with S-cyclins initiates DNA replication (Epstein and Cross, 1992; Morgan, 2007). The presence of both recognition site and cyclin docking motif will affect Cdc28 target specificity.

Consensus motif

Cdc28 is a serine/threonine-protein kinase, but the affinity of the kinase to the phosphorylation sites is determined by the amino acids surrounding the serine or threonine residue. Due to the presence of a hydrophobic pocket near its active site, Cdc28 has higher affinity to

phosphorylation sites with Pro at +1 position. The so-called full consensus motif for Cdc28 phosphorylation is [S/T*]Px[K/R], where S/T* is an amino acid being phosphorylated[1].

The intrinsic activity of Cdc28 grows as the cell cycle progresses. It was found that cyclins not only activate Cdc28 but change its specificity towards the consensus motif (Kõivomägi et al., 2011b; Loog and Morgan, 2005a). This specificity gradually rises through the cell cycle, and in M-phase Cdc28-Clb2 can phosphorylate site at a minimal consensus motif [S/T*]P without adjacent K/R residues (Kõivomägi et al., 2011b; Morgan, 2007).

Cyclin docking motifs

Apart from modulating intrinsic activity towards the consensus motif (which is recognized by Cdc28 itself) cyclins also recognize and bind short linear motifs on the substrate proteins. These motifs are called cyclin docking motifs. Cyclin binding to the target protein allows tighter contact of substrate and cyclin-Cdc28 complex (Figure 1). The first discovered docking motif was RxL docking motif (broadened to [R/K]xLφ or [R/K]xLxφ), which binds to hydrophobic patch in S-cyclin Clb5 and less in M-cyclin Clb3 (Kõivomägi et al., 2011b; Loog and Morgan, 2005b).

Some Cdc28-cyclin complexes have low specificity even towards the full consensus motif, and yet show high specificity towards their targets. For example, some Cdc28 targets are phosphorylated the most during the Cdc28-Cln1/2 maximal levels, even though these complexes show very low full consensus motif specificity in comparison to other Cdc28-cyclin complexes (Kõivomägi et al., 2011b; McCusker et al., 2007). This suggested that Clb5 is not the only cyclin with the ability to bind substrate. Indeed, in recent years docking motifs that interact with a hydrophobic patch or other regions of cyclins were discovered for three major cyclin types. For G1/S-cyclins Cln1/2 it is VLxxPφxφ, or LP motif (Bhaduri and Pryciak, 2011; Köivomägi et al., 2011b), for S cyclin Clb5, as mentioned above, RxL motif, for early G2/M-cyclin Clb3 it is PxxPxF, or PxF motif (Örd et al., 2020) and for late G2/M-cyclins Clb1/2, it is LxF motif (Örd et al., 2019a).

Some Cdc28-cyclin substrates have multiple docking sites. Sic1, for example, contains docking motifs for different cyclins (LP and RxL). Moreover, it has several docking motifs of the same kind (four RxL sites at different regions of polypeptide chain). It was shown that in the

[1] In sequence motif representation, [X/Y] means „either X ot Y“, x means „any amino acid“, φ means “any hydrophobic amino acid”. Amino acids are written as their one-letter abbreviations.

case of multiple docking motifs, each motif is important for phosphorylation of a specific site or a group of closely located sites (Kõivomägi et al., 2011b). In addition, the distance between the docking motif and the phosphosite affects the phosphorylation rates, with optimal distances varying between cyclins (Kõivomägi et al., 2013).

1.4 Protein degradation in cell cycle regulation

As was mentioned above, oscillations of Cdc28-cyclin complexes levels are directly connected with the fluctuations of cyclin levels. Thus, regulation of cyclin abundance in the cell plays a significant role in the cell cycle control system. It happens at multiple levels.

The first level is the expression of cyclin-encoding genes. Gene expression is controlled through transcriptional factors, molecules that influence RNA polymerase affinity to the promoter region. Transcription factors, which control the expression of cyclins, are themselves activated as a consequence of cell cycle events occurred in the previous stage, which contributes to the correct ordering of the cycle and ensures its further progression. For example, the expression of *CLN1,2* genes is controlled by the SBF transcription regulation complex, which is inactivated by association with Whi5 protein. The Cln3-Cdc28 performs inhibitory phosphorylation of Whi5, releasing SBF and leading to the expression of *CLN1* and *2* (Morgan, 2007).

The second level of the regulation of cyclin abundance during the cell cycle is the control of their degradation rates. Transition between cell cycle phases, as well as drop in the cyclin levels happen within a timeframe of a few minutes (Kõivomägi et al., 2011b). Thus, cyclins involved in the regulation of the previous stage have to be degraded in a short time period to ensure correct cell cycle progression.

The degradation rates of cyclins and other cell-cycle regulators is controlled by ubiquitin-dependent proteolysis. In this proteolytic pathway, proteins must be ubiquitylated to be recognized and processed by huge protease complexes – proteasomes. Ubiquitin tagging is performed in three steps by three types of enzymes — E1, E2, and E3 (corresponding to the number of catalyzed steps). E1, ubiquitin activator, binds ubiquitin and then interacts with ubiquitin-conjugating enzyme E2, which catalyzes the transfer of ubiquitin to the E2 active site. Finally, E3, ubiquitin-protein ligase, mediates the transfer of ubiquitin from E2 to a target protein.

There are several ubiquitin-protein ligases, but two of them are especially important for cell cycle regulation. The first one is the anaphase-promoting complex (APC), which facilitates

the metaphase-to-anaphase transition. The second one is a multisubunit enzyme complex called SCF, responsible for marking Sic1, Far1, and G1/S cyclins for degradation in the early S phase (Morgan, 2007).

SCF consists of the following subunits: Cul1 (cullin), Rbx1 (domain where conjugate E2-ubiquitin binds), Skp1 with an associated F-box protein. F-box proteins bind target proteins and therefore determine SCF specificity (Skowyra et al., 1997). F-box proteins involved in the degradation of G1 inhibitors and G1/S cyclins are Cdc4 and Grr1, respectively. However, there is some overlap in substrate specificity as Cdc4 can target some of the G1/S cyclins. Thus, different substrate specificity of Grr1 and Cdc4 is partially determined by localization of F-box proteins — SCF^{Cdc4} can be found mainly in the nucleus (along with Sic1 and Far1), while SCF^{Grr1} is in the cytoplasm, where G1/S cyclin-Cdc28 complexes are located (Landry et al., 2012).

Degrons

Some proteins carry distinct regions important for the regulation of their degradation rates. These regions are called degrons. For APC and SCF targets, degrons are the regions recognized by these complexes. The most common APC-recognized degrons are D-box (destruction box, motif RxxLxxxN) and KEN-box (motif KENxxxN) (Morgan, 2007). The majority of degrons in SCF-targeted proteins are recognized by F-box proteins only after phosphorylation of certain sites inside targets' amino acid sequence (Feldman et al., 1997; Skowyra et al., 1997). Degrons like these are called phosphodegrons (Holt, 2012). In the cell cycle of *S. cerevisiae*, this conditional degradation contributes to the ordering of the cell cycle. For example, Sic1, which acts as S- and M-complexes inhibitor, is phosphorylated and targeted for degradation by G1/S- and, later, S- cyclin-Cdc28 complexes, allowing the cell cycle to proceed.

A large amount of CDKs targets carry more than one phosphosite and they are usually located in intrinsically disordered regions of proteins (Holt et al., 2009; Tyanova et al., 2013). This makes phosphodegrons a valuable tool for synthetic biology, because phosphodegron can be fused to a protein without affecting its tertiary structure, and can perform the same function as in the source polypeptide – protein degradation (Jakubowski and Spinali, 2017). Phosphodegrons were previously transferred from one protein to another to achieve destabilization (Mateus and Avery, 2000) or study the nature of degrons themselves (Faustova et

al., 2021; Gordley et al., 2016; Örd et al., 2019b). In the case of SCF-targeted degrons, combinations of priming sites, phosphodegron sites, and docking motifs can be used to adjust desired degradation timing for the protein (Örd et al., 2019b).

Targeted protein degradation

The ability to regulate levels of a specific protein in the cell can be useful in many ways. For example, knockout/knockdown mutants are widely used in research to study protein functions. In metabolic engineering, downregulation of the brunching reactions is often applied to increase the metabolic flux towards the target pathway. This desired downregulation can be applied at several levels. Indirect ways for protein regulation include deletion of the gene from the genome, transcriptional regulation, and control using RNA interference (Blazeck et al., 2012; Elbashir et al., 2001; Hegemann and Heick, 2011; Jensen et al., 2017; Ottoz et al., 2014). Control of degradation, protein inactivation or relocation are among direct approaches used for the regulation of protein abundance (Contegno et al., 2002; Niopek et al., 2014; Nishimura et al., 2009).

Conditional and rapid protein downregulation is crucial for both research and engineering applications. It is especially important in the case of essential proteins when knockout mutants are not viable or possess significant growth defects. Inducible protein degradation allows of the assessment of the immediate consequences of protein depletion on the cell fate or the fast switching to active production of desirable product. The efficiency of indirect ways of 'switching off' the protein, such as regulation of transcription or RNA interference, would still depend on protein degradation rates, as already existing protein molecules will stay in the cell and be active degraded. Therefore, direct control of protein levels could be more advantageous for some applications (Wu et al., 2020). Among direct methods of the regulation of protein abundance, protein fusion with a phosphodegron tag could enable fast and conditional protein degradation without interference with protein structure.

2 THE AIMS OF THE THESIS

The main aim of the thesis was to optimize the Sic1-Cln2-based Cdk1-Clb3 degron tag for the inducible targeted protein degradation. This aim consists of subtasks:

- To reconstruct inducible targeted protein degradation system previously developed in our lab to ensure that system is replicable and establish a workflow for protein tagging using CRISPR/Cas9 system.
- To study the effect of Grr1 promoter exchange.
- To optimize Sic1-Cln2 based Cdc28-Clb3 targeted degron tag.

3 EXPERIMENTAL PART

3.1 MATERIALS AND METHODS

3.1.1 Materials

Media

Following media were used for growth and selection of bacterial and yeast cultures:

LB (lysogeny broth) media: 10 g/L tryptone, 5 g/L microgranulated yeast extract, 10 g/L NaCl. Selection plates: LB agar plates with addition of 100 mg/L of either ampicillin or kanamycin.

YPD (Yeast Extract–Peptone–Dextrose) media: 20 g/L peptone, 10 g/L micro granulated yeast extract, 20 g/L D-Glucose anhydrous.

CSM (Complete Supplement Mixture): 20 g/L peptone, 10 g/L CSM. Selection plates: G418 CSM agar plates (200 mg/L G-418 and 20 g/L D-Glucose anhydrous) and LEU dropout CSM plates (CSM, -LEU instead of the complete CSM and 20 g/L D-Glucose anhydrous).

For agar plates preparation from a certain liquid media, 15 g/L of agar was added to a media mixture.

Bacterial strains

Competent Turbo E. coli cells prepared in our laboratory were used for the molecular cloning.

Yeast strains

Table 1. Yeast strains implemented in this project.

Strain	**Degron tag**	***GRR1* promoter**
RKI450 RKI451 RKI452	TTT STST 2×PxF Sic1C	Endogenous
RKI453	TTT AAAA 2×PxF Sic1C	
RKI456	No degron, no mCherry	
RKI514	No degron, no mCherry	Inducible *GAL1* promoter

Strain	**Degron tag**	***GRR1* promoter**
RKI521	TTT AAAA 2×PxF Sic1C	
NS352	No degron, mCherry integrated	
NS354 NS355	TTT STST 2×PxF Sic1C	
NS358 NS359	TTT STST 2×PxF	
NS364 NS365	TTT ST(-3)ST 2×PxF Sic1C	
NS366 NS367	TTT ST(-9)ST 2×PxF Sic1C	
NS368 NS369	TT(-9)T STST 2×PxF Sic1C	
NS370 NS371	TTT STST PxF(-5)PxF Sic1C	
NS372 NS373	TTT STST PxF	
NS374 NS375	TTT STST PxF GSA linker	
NS376 NS377	T STST 2×PxF Sic1C	
NS378 NS379	STST 2×PxF Sic1C	
NS391 NS392 NS393	TTT STST 2×PxF Sic1CΔ74	

Yeast strains are MATa haploids of the W303 strain. Strains, constructed in this study, were generated with lithium acetate mediated transformation (see Methods section). Strains with 'RKI' starting number were taken from the library of Rait Kivi, other strains in the table were created for this study. All strains used and created in this work share three genetic modifications: LexA-ER-B112 transcription factor coding sequence under the constitutive *ACT1* promoter in *his3* locus, truncated Clb3 fused to NES and EGFP coding sequence under

the synthetic inducible pEstr promoter (Fig. 3) in *ura3* locus and endogenous *CLB3* gene deletion. If mCherry is integrated, it is constitutively expressed under *ADH1* promoter, carries NES signal on the N-terminus and is tagged with 3xHA tag from the C-terminus; degrons are inserted between NES and mCherry (Fig. 3). Genotypes of all strains are described in Supplementary Table 1.

Plasmids

Plasmids used in this study are listed in the Tables 2&3. Table 2 contains standard plasmids (vectors) used in this study to build DNA constructs. Table 3 contains plasmids, constructed for this project.

Table 2. Standard plasmids used in this study.

Plasmid	**Short description**	**Source/ Reference**
pUC18	Cloning vector for the expression in *E. coli*	Norrander, Kempe, & Messing, 1983
pWS173	Cas9-sgRNA gap repair vector, *KanR* (*G418*) yeast selection marker	Tom Ellis lab (Addgene plasmid #90516; http://n2t.net/addgene:90516 RRID:Addgene_90516)
pWS082	sgRNA entry vector	
pRG205mx	Integrative *E. coli*/*S. cerevisiae* shuttle vector, *LEU2* selection marker	Gnügge, Liphardt, & Rudolf, 2016

Table 3. Standard plasmids used in this research. All plasmids used in this study except for pWS173 carried *AmpR* selection marker, and in pWS173 *KanR* is used as both bacterial and yeast selection marker.

Plasmid	**Cloning vector**	**Insert or degron tag (for pNS157-derived plasmids)**	**Primers for oligonucleotide-directed mutagenesis used to create the plasmid***
pRKI121**	pRS305	pADH1-NES-Degron tag(TTT STST 2×PxF Sic1C)-mCherry-3HA	-
pRKI141***	pRS305	pADH1-NES-Degron tag(TTT AAAA 2×PxF Sic1C)-mCherry-3HA	-
pNS129	pRG205mx	pADH1-NES-mCherry-3HA-tCYC1	-
pNS143	pWS082	sgRNA for mCherry N-terminus targeting	-

Plasmid	Cloning vector	Insert or degron tag (for pNS157-derived plasmids)	Primers for oligonucleo-tide-directed mutagenesis used to create the plasmid*
pNS155	pUC18	pADH1(106 bp****)-NES-Degron tag(TTT STST 2×PxF Sic1C)-mCherry(107 bp****) amplified from pRKI121	-
pNS157	Based on pNS155, at PAM site synonymous single-point mutations are introduced	pADH1(106 bp)-NES-Degron tag(TTT STST 2×PxF Sic1C)-mCherry(107 bp, mutated PAM sites)	6379/6378
pNS161	Based on pNS157, degron tag sequence al-tered by site-directed mutagenesis	TTT ST(-3)ST 2×PxF Sic1C	6500/6499
pNS164		TTT ST(-9)ST 2×PxF Sic1C	6504/6503
pNS166		TT(-9)T STST 2×PxF Sic1C	6512/6511
pNS167		TTT STST PxF(-5)PxF Sic1C	6508/6507
pNS172		TTT STST PxF	6535/6505
pNS174		TTT STST 2×PxF	6535/6509
pNS176		TTT STST PxF-GSA linker	6534/6506
pNS178		TTT STST 2×PxF-GSA linker	6534/6510
pNS180		T STST 2×PxF Sic1C	6685/6684
pNS182		STST 2×PxF Sic1C	6686/6684
pNS184		TTT STST 2×PxF Sic1CΔ74	6805/6804

* For the amplification of donor DNA fragments for mCherry N-terminus tagging from degron tag carrying plasmids, primers 6388 and 6389 were used, and final lengths of homol-ogous flanking regions for the insert are 140 bp from 5'- and 124 bp from 3'-end. To amplify insert from pRKI121 and pRKI141 for subcloning into pUC18, primers 6173 and 6175 were used.

, * pRKI121 and pRKI141 were constructed by the member of our lab, PhD Rait Kivi. All other plasmids were constructed for this study.

**** Plasmids containing degron variants contained not full-length pADH1 and mCherry sequences, but degron flanking regions of about 100 bp.

Primers

All primers used in this study are listed in Supplementary table 2.

3.1.2 PCR

Fragments for insertion into pUC18 and donor DNA fragments for CRISPR genome editing were amplified using Phusion polymerase (2 U/μL) and 5xHF buffer (Thermo Fisher Scien-tific).

For yeast colony PCR, yeast single colonies from agar plate were lysed by boiling cells suspended in 20 mM NaOH solution. After lysates' centrifugation, 1 µl of supernatant was used as DNA template in PCR reaction. Reaction mixes were prepared using 5xHOT FIREPol® MultiPlex Mix Ready to Load (Solis Biodine).

For Phusion reactions, denaturation temperatures were both 98 °C, annealing temperature was calculated by adding 3 °C to the lower melting temperature from the pair of primers, and elongation time was calculated as 30 seconds per kilobase. For FIREPol reactions, denaturation temperatures were both 95 °C, lower melting temperature from the pair of primers was used as an annealing temperature, and elongation time was calculated as 1 minute per kilobase.

3.1.3 DNA cloning

All used restriction enzymes and buffers were Thermo Fisher Scientific Fast Digest. For all ligation reactions, T4 DNA Ligase (5 U/µL) and 10xT4 DNA Ligase Buffer from Thermo Fisher Scientific were used, and if ligase or ligation buffer is mentioned it refers to these products. 1:3 insert:vector ratio was used for all ligation reactions.

To create the plasmid for mCherry genomic integration, NES-mCherry-3xHA PCR fragment (amplified from pRKI121 with 6080/6180 primers) and pRG205mx cloning vector were digested with BamHI and Cfr42I restriction enzymes and mixed for ligation. After the bacterial transformation and plasmid extraction (Favorgen plasmid extraction mini kit according to the protocol provided by manufacturer), pRG205mx-NES-mCherry-3xHA and unlabeled pRS305-PADH1-tCYC1 plasmid were digested with Cfr42I and SacI, and tCYC1 was ligated into pRG205mx-NES-mCherry-3xHA, transformed and purified, resulting in pRG205mx-NES-mCherry-3xHA-tCYC1. The last step was the digestion of pRG205mx-NES-mCherry-3xHA-tCYC1 and same unlabeled pRS305-PADH1-tCYC1 plasmid with EcoRI and BamHI and subsequent ligation of PADH1 into the construct. The result was pRG205mx-PADH1-NES-mCherry-3xHA-tCYC1 plasmid, which was labelled as pNS129.

To clone degron constructs with flanking regions into pUC18, regions of interest were PCR-amplified from pRKI121 and pRKI141 and directly ligated into pUC18 previously restricted with *SmaI* (FastDigest, Thermo Fisher Scientific). For ligation reactions, T4 DNA Ligase (5 U/µL, Thermo Fisher Scientific) and 10xT4 DNA Ligase Buffer (Thermo Fisher Scientific) were used.

SgRNA plasmids were cloned using the Golden Gate assembly method with *BsmBI* type II restriction enzyme. Prior to the assembly, 5'- to 3'- and 3'- to 5'- strands of guide fragment (the insert to pWS082 standard plasmid) were phosphorylated by T4 Polynucleotide Kinase (10 U/µL, Thermo Fisher Scientific) to allow ligation and annealed using thermocycler by holding them at denaturation temperature of 96 ℃ and then slowly (0.1 ℃ per second) cooling down to 23 ℃ (Shaw). 2 µL of annealed oligos were mixed with 0.5 µL of pWS082, 1 µL of *BsmBI*, 1 µL of ligase and ligase buffer in 10 µL reaction.

3.1.4 Site-directed mutagenesis

Site-directed mutagenesis of plasmids was used to introduce both deletions and single-point mutations (removing PAM sites from the donor DNA to avoid CRISPR/Cas9 complex cutting on it after the successful recombination). To insert desired changes, primers for the inverse PCR were designed in back-to-back orientation. In the case of deletion, primers flank the deletion region. For mutagenesis, primer/s possessed the desired mutations at their 5'-ends. Primers were designed to have a melting temperature near 70°C. Site-directed mutagenesis was performed using Phusion polymerase (2 U/µL) and 5xGC buffer (Thermo Fisher Scientific). Thermocycler settings were similar to standard PCR amplification described above, with the difference that annealing temperature was 70°C for all reactions. After acquiring PCR product, around 50 ng of it was mixed with 10xT4 DNA Ligase Buffer (Thermo Fisher Scientific), 1 µL of T4 Polynucleotide Kinase (10 U/µL, Thermo Fisher Scientific), and 1 µL of *DpnI* (Thermo Fisher Scientific Fast Digest) in 20 µL reaction and incubated for 30 minutes at 37°C. After that, 1 µL of T4 DNA Ligase (5 U/µL, Thermo Fisher Scientific) was added directly to the mix, which was subsequently incubated for 10 minutes at room temperature and transformed to *E. coli*.

3.1.5 Bacterial transformation

Competent Turbo *E. coli* cells were kept at -80°C. Prior to addition of DNA, cells melted to liquid on ice. 50 µL of competent cells were used per transformation. 2 µL of ligation mixture were added to the cells and gently resuspended. Resulting mixture was kept on ice for 30 minutes. After that, heat shock was applied to the mixture by incubating it for 40 seconds at 42°C, and cells were chilled on ice for 2 minutes. The transformation mixture was then diluted with 500 µL of LB media and incubated for 30 minutes in 220 rpm shaker at 37°C. After incubation, the cells were precipitated by centrifugation at 6000 rpm for a minute. 350 µL of the supernatant was removed and the pellet was resuspended in the rest of the media.

Cells were then plated on LB agar plates with proper antibiotic and incubated for 12-15 hours at 37°C.

3.1.6 Lithium acetate-mediated yeast transformation with CRISPR genome editing

For transformations, 50 mL of yeast culture at optical density 0.6-0.8 at 600 nm was centrifuged for 2 min at 2000 rpm to collect cells. The cell pellet was resuspended in 1 mL of sterile 100mM solution of lithium acetate in TE buffer (10 mM Tris, 1mM EDTA) and centrifuged again at 3600 rpm for 1 minute. The supernatant was removed, and cell were resuspended in 100mM LiAc in TE buffer that exceeded cell volume approximately two times. Yeast competent cells were incubated at room temperature for 10 minutes. In parallel, salmon sperm DNA was boiled for 10 minutes at 100 ℃ and was put on ice to chill immediately after to keep DNA single-stranded (SS-DNA). 10 µL of SS-DNA were then mixed with DNA to be transformed: in case of integration plasmids transformations, it was 200-500 ng of linearized plasmid, and in case of CRISPR/Cas9 transformations it was 200 ng of sgRNA plasmid linearized with *Eco32I*, 100 ng of Cas9-carring vector linearized with *Esp3I* and around 2 µg of donor DNA. 100 µL of yeast competent cells were added to the DNA mixture. Next, 700 mL of sterile PEG/LiAc solution (40% PEG 3350 + 100 mM LiAc in 1x TE) and 48 µL of DMSO were added and gently mixing by pipetting up and down. The mixture was incubated at 42 ℃ for 40 min and after the incubation was chilled on ice for 2 minutes and centrifuged for 1 minute at 6000 rpm. The supernatant was removed, and pellet was resuspended in 1 mL of sterile 1xTE buffer for washing and centrifuged for 2 minutes at 2000 rpm. The supernatant was removed, and cells were resuspended in 200 µL of sterile 1xTE buffer and plated on the agar plates. In case of *URA3* and *LEU2* selection markers, cells were plated directly to dropout plates, but in case of G-418 selection they were first plated to YPD, grown overnight at room temperature and the next day replica plating to G-418 containing CSM plates was performed.

3.1.7 Time-lapse fluorescence microscopy

For time-lapse microscopy experiments, CSM media with the addition of sugars as carbon sources was used. Sugar solution stocks (20%) were diluted 10 times in CSM media, resulting in a 2% final sugar concentration. To prepare agarose pads, low melting temperature

agarose (NuSieveTM GTGTM Agarose) was melted in the medium (final agarose concentration was 2%). Both media and melted agarose were filtered through a 0.20 μm pore filter (GVS Filter Technology) before use.

Yeast cultures were grown at 30 °C in synthetic complete media with 2% of sugar (raffinose or glucose) to OD 0.2–0.6. Cells were pipetted onto 0.8-mm cover glass slips and covered with a 1-mm thick 2% agarose pad made with a proper medium.

Microscopy was performed with a Zeiss Observer Z1 microscope with a 63×/1.4NA oil immersion objective and an Axiocam 506 mono camera (Zeiss). 3 × 3 pixel binning was used for imaging. Throughout the experiment, the temperature of the agarose pad was kept at 30 °C using a Tempcontrol 37–2 digital (PeCon). Images were taken every 3 min, and imaging sessions were 3 h long. Up to 27 positions were imaged in one experiment using an automated stage and ZEN software. Definite Focus was used to keep the cells in focus during the experiment.

Following exposure settings were used for experiments: 25 ms exposure time for phase contrast channel, 15 ms for EGFP channel, 750 ms for the mCherry channel. Colibri 470 LED module and Colibri 550 LED module at 25% intensity were used as excitation light sources for EGFP and mCherry imaging, accordingly.

3.1.8 Western blot

The reporter protein mCherry with nuclear export signal and degron tag from N-terminal and a C-terminal 3xHA tag was expressed under the *ADH1* promoter. The Grr1 and an N-terminal 3xHA tag was expressed under inducible promoters, either *GAL1* promoter or pEstr. For western blotting, liquid cultures with OD 0.2-0.4 were diluted in 50 mL to OD 0.05-0.1 and grown for around 8 hours until OD 0.3-0.4, all in CSM with glucose (strains with *GRR1* under pEstr) or raffinose (strains with *GRR1* under *GAL1* promoter). Cultures were induced with 1μM β-estradiol and/or addition of the galactose (final concentration in culture 2%). For sample collection, 5 mL of culture were centrifuged at 4000 rpm for 1 minute every 10 minutes, supernatant was removed, sample was frozen in liquid nitrogen and then stored at -80 °C. Cells were lysed by bead beating in lysis buffer containing urea. Proteins were separated using SDS-PAGE with 8% (Grr1 experiments) or 10% (mCherry experiments) acrylamide. Blotting of SDS-PAGE gels was performed using a Power Blotter–Semi-dry Transfer System (Thermo Fisher Scientific). Purified anti-HA epitope tag antibody (1:500) (clone 16B12, BioLegend Cat. No. 901501) and HRP-conjugated anti-mouse antibody (1:7.500)

from Labas, Estonia were used to detect the 3HA-tagged proteins. SuperSignal™ West Pico PLUS Chemiluminescent Substrate kit (Thermo Fisher Scientific) was used to acquire signal.

3.1.9 Quantitative analysis of the time-lapse microscopy data

Image segmentation, cell tracking, quantification of fluorescence signals and statistical analysis was performed using MATLAB (The MathWorks, Inc.). Scripts used originate from Doncic et al., 2013.

For statistical analysis, we kept only cells that met a set of conditions and filtered out the rest. It was done to exclude cells that appeared later in experiments through cellular division (no signal in first 15 minutes), dead cells (cells showing high and stable fluorescence levels for both EGFP and mCherry from the start of the experiment), cells with outstandingly low levels of mCherry in the beginning of the experiment and of EGFP levels in the end. On average, around 30% of cells were filtered out from every sample, majority of them due to late appearance. We also subtracted background from cell fluorescence values. Background was calculated as arithmetic average of signal intensities of cells without expression of fluorescent proteins EGFP and mCherry.

In figures showing normalized mean fluorescence intensities, each cell was normalized to its maximal fluorescence value. After that, individual cells were synchronized so that at 0 timepoint fluorescence level of mCherry is halfway from its maximal value to the minimal one for this cell. It was done to synchronize cells considering uneven distribution of inducer in the solid media. In figures showing non-normalized data (Figure 4D, 5 and 7C), there is no synchronization. Mean value was calculated as arithmetic mean for all of the samples. The error bars for all plots are ± standard error mean (s.e.m.) from the single-cell fluorescence sample set.

3.2 RESULTS AND DISCUSSION

In this study, we aimed to develop a set of phosphodegron tags based on the system previously designed in our laboratory (ongoing project, data unpublished). This system allows cell-cycle independent, inducible, cytoplasmic degradation of the target proteins (protein-of-interest, POI). It consists of the inducible input and the POI. In this work, we used mCherry as a reporter to visualize the degradation of POI. The input has two components, both are under inducible promoters: 1) truncated Clb3 fused to Nuclear Export Signal (NES) and EGFP from N- and C-terminus, respectively, under inducible synthetic promoter pEstr (pEstr-NES-Clb3Δ130-EGFP, induced by β-estradiol; this construct is also referred to as 'kinase input'); 2) Grr1 tagged in the endogenous locus with N-terminal 3xHA-epitope tag and placed under control of *GAL1* promoter (pGAL1-3xHA-Grr1, induced by galactose) (Figure 3). To ensure cytoplasmic localization of mCherry reporter NES sequence was fused to its N-terminus. Phosphodegron tags were inserted between NES and mCherry. The mCherry reporter expression was under control of the strong constitutive ADH1 promoter (Figure 3).

Clb3 is one of the cell cycle regulators functioning mainly in the nucleus, and one of the aims was to make the system cell cycle independent. It was achieved by cytosolic expression of otherwise nuclear Clb3 (Bailly et al., 2003). In addition, first 130 N-terminal amino acids sequence containing D-box, which regulated Clb3 abundance, were deleted. D-box deletion made Clb3 stable since it cannot be recognized by APC (Pecani and Cross, 2016). Indeed, Clb3Δ130 levels are stable during 8-hour experiment (data not shown). Endogenous Clb3 was deleted to prevent its action in the cytoplasm, which would lead to undesirable degradation before the induction of input expression. Since Clb cyclins are redundant and have significant functional overlap (Cross and Yuste-Rojas, 1999), Clb3 deletion was not expected to affect the cell cycle.

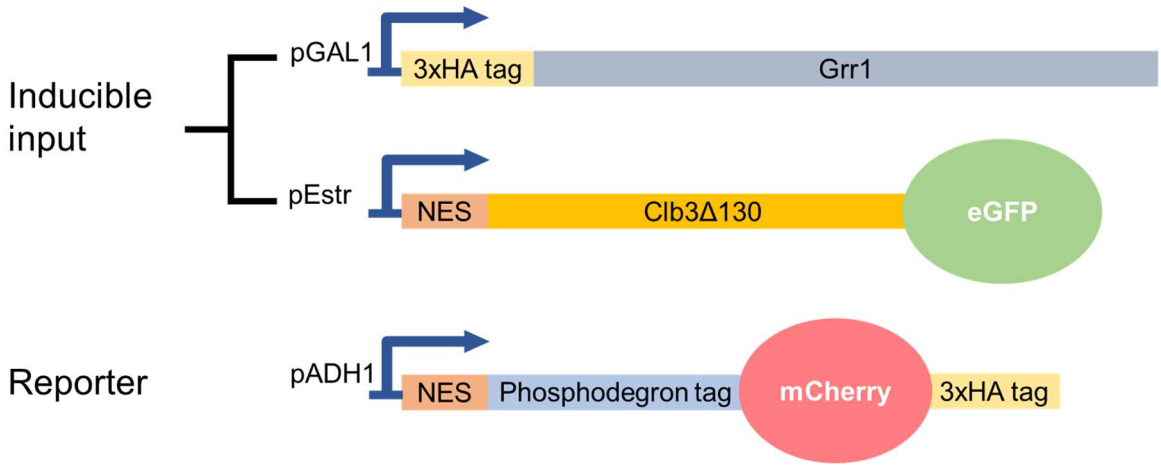

Figure 3. Schematic representation of inducible targeted degradation system (Figure was adapted from Rait Kivi, unpublished). Inducible input consists of truncated stable cyclin Clb3Δ130 expressed in the cytoplasm due to NES fusion and F-box protein Grr1. EGFP was fused to NES-Clb3Δ130 to visualize its expression and estimate the stability of the kinase input. Fluorescent protein mCherry was used as a model protein of interest for tagging with a phosphodegron. mCherry was expressed from a strong constitutive ADH1 promoter. Phosphodegron efficiency was estimated based on the decline in mCherry fluorescence after input induction. NES was added to guarantee cytoplasmic localization of mCherry. 3xHA tag was used to allow analysis of protein levels by Western Blotting.

3.2.1 Full-length TTT STST 2×PxF phosphodegron tag

A full-length phosphodegron tag (FL), TTT STST 2×PxF Sic1C, was designed based on the sequence of the Sic1 (Rait Kivi, unpublished). The last 69 aa were removed, as it is an Cdc28 inhibitory domain (Hodge and Mendenhall, 1999). As the system should be active in cytoplasm, native phosphodegron of Sic1 (45-80 aa, Figure 1), which is recognized by nuclear SCF^{Cdc4}, was replaced with phosphodegron from Cln2 (393-445 aa fragment of Cln2 cyclin) (Berset et al., 2002) recognized by cytoplasmic SCF^{Grr1}. Three native docking motifs (the first and the last RxLs and the only LP) were mutated to alanines. Second and third RxL motifs were replaced with PxF to make the phosphodegron tag Clb3-Cdc28 specific. In the region 120-215 aa of Sic1, phosphosites were mutated to alanines, and this region was used as a flexible linker between the protein of interest and phosphodegron tag. This linker is referred to as Sic1C or Sic1C linker throughout this work. The FL phosphodegron tag can be logically divided into four modules: Cks1 priming module (1-44 aa, contains T2, T5 and T33 phosphosites originating from Sic1), phosphodegron module (45-97 aa, contains S48, T57, S79 and T82 phosphosites, which are part of Cln2 degron), Clb3 docking module (98-132 aa, contains two Clb3-specific PxF docking sites), and Sic1C linker (Figure 4A).

As we aimed to test several phosphodegron variants, we first constructed a strain with constitutively expressed pADH1-mCherry-3HA (single-copy insertion was ensured by using a method from Gnügge et al., 2016) and inducible input (Figure 3). This strain was used as a background strain for further tagging with all new degron variants. mCherry phosphodegron tagging was performed using CRISPR/Cas9 system. In contrast, in previously constructed strain mCherry was inserted into the genome already carrying a tag, as part of integrative vector (Rait Kivi, unpublished).

We compared new NES-FL-mCherry strains with previously existed ones in the same conditions to compare degradation rates and test results reproducibility. To check protein degradation profiles, single-cell fluorescent microscopy was used. The degradation rates of old and new strains were similar, with tagged mCherry reaching half of its peak fluorescence in around 25 minutes (Figure 4B, estimated from the graph). In the absence of inducible input, tagged mCherry was stable (Figure 4B). To prove the role of phosphorylation in the degradation of the tagged protein, we tested strain carrying tag with all phosphosites in the phosphodegron module (Figure 4A, green) mutated to alanines (cannot be phosphorylated by Cdc28). The results show that alanine mutants were stable under all tested conditions, including input induction (Figure 4D). It was concluded that phosphodegron tagging can be performed with CRISPR/Cas9, which enables tagging of proteins without integrating selective markers into the genome. In addition to that, we showed that the results are highly reproducible, with degradation rates of the protein similar to that in the previously generated strains carrying the same tag (Figure 4B). The same can be concluded based on the comparison of biological replicates (data not shown).

In addition, we confirmed that Cks1 module alone with 2×PxF phosphosites does not contribute to degradation (strains with mutated phosphodegron phosphosites do not change their fluorescence under any conditions tested, although they possess untouched Cks1-priming and cyclin docking modules, Figure 4C, D). These findings are in agreement with previous research on the role of Cks1 in protein phosphorylation (Berset et al., 2002; Kõivomägi et al., 2011a).

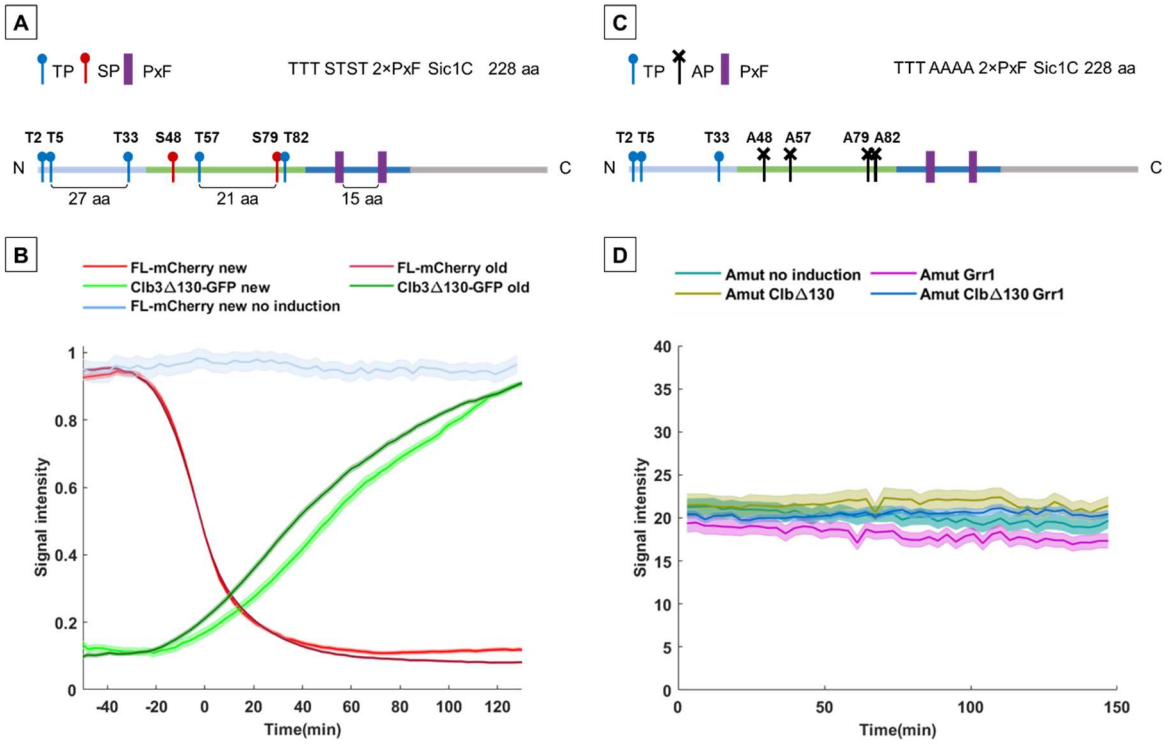

Figure 4. Full-length degron characterization. **A**, The schematic representation of the full-length (FL) degron used to tag mCherry in strains used for microscopy in **B**. It is logically divided into Cks1-priming module (light blue), phosphodegron module (green), cyclin docking module (dark blue), and Sic1C linker (grey). The same color-coding is used for all degron tag variants. Numbers below the scheme show distances in between elements (phosphosites and docking motifs). **B,** Plot showing synchronized, normalized to maximum, mean cytoplasmic levels of tagged mCherry (red lines, blue line) and Clb3Δ130-EGFP (green lines) in old (previously constructed in our lab) and new (generated for this study) strains. **C**, The schematic representation of the FL phosphodegron module with phosphosites mutated to alanine. It was used to tag mCherry in strains used for microscopy in **D**. **D**, Plot showing mean cytoplasmic levels of mCherry tagged with alanine-mutated FL degron with no induction, partial induction (either Grr1 or Clb3Δ130) or full induction (with both Grr1 and Clb3Δ130 in parallel). For both **B** and **D**, the error bars are ± standard error mean (s.e.m.) from the single-cell fluorescence sample set.

3.2.2 Grr1 expression from the native promoter leads to the degradation of the tagged protein even in the absence of Clb3Δ130 input

Grr1 conditional expression requires the replacement of the native *GRR1* promoter. The lack of Grr1 in the cell would theoretically lead to an excessive accumulation of Grr1 substrates, for example, Cln2. Based on our previous experience, we know that Cln2 overexpression is not lethal for the cell but leads to morphological changes and prolongs G1 phase (unpublished data). At the initial stages, we checked possibility to keep Grr1 under its native promoter and to simplify the design of the system by that mean. So, we compared levels of

FL-tagged mCherry in the strains with either endogenous or conditional expression of Grr1 under inductive and non-inductive conditions. The results show that the presence of Grr1, when it was endogenously expressed at low levels (Flick and Johnston, 1991), led to substantially reduced fluorescence of tagged mCherry, even in the absence of Clb3Δ130 (Figure 5).

These results can be explained by the fluctuations of the intrinsic activity of Cdc28 towards its targets during the cell cycle. One of the phosphosites in the degron module, T57, is a full-consensus motif, which should be phosphorylated early in the cell cycle regardless of cyclin-specific docking motifs. The other three phosphosites in the degron are minimal consensus motif phosphosites, which can be phosphorylated later, in G2, when Cdc28 complexes have higher intrinsic activity towards them (Morgan, 2007; Örd and Loog, 2019). It means that even in the absence of Clb3, FL-mCherry can be phosphorylated and send for degradation in the presence of Grr1. Thus, endogenous *GRR1* expression results in constantly low levels of tagged protein in the cells. Without Clb3Δ130 input, the level of mCherry fluorescence in the strain with endogenous Grr1 was only a bit higher than in the case of degraded mCherry in the strain conditionally expressing Grr1 after induction (Figure 5).

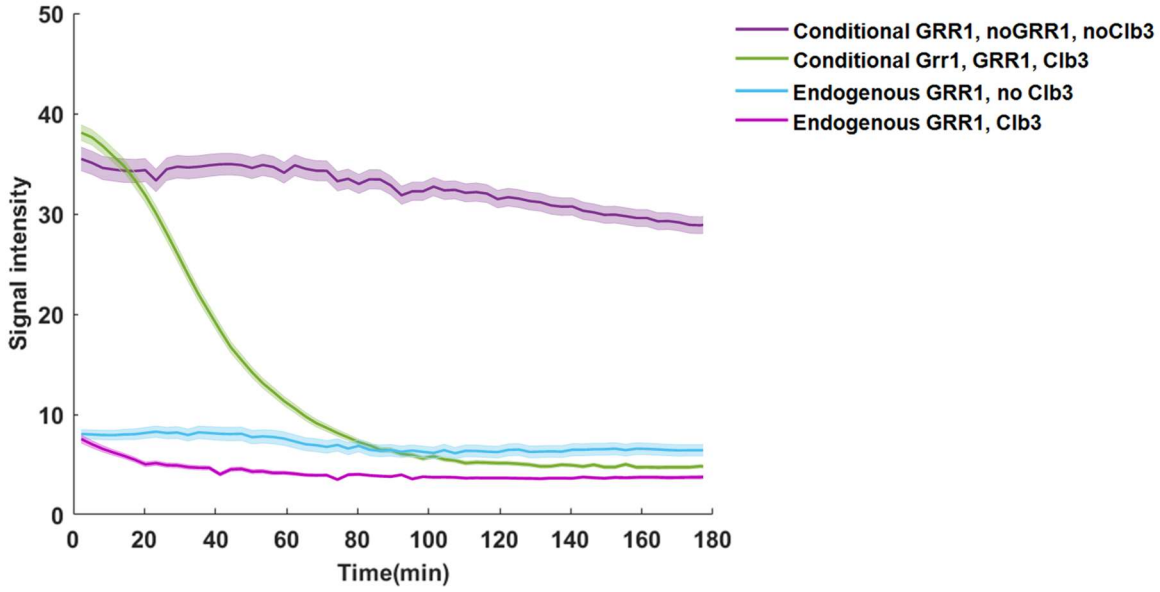

Figure 5. Plot showing mean cytoplasmic FL-mCherry levels with and without Clb3Δ130 induction in strains with Grr1 under either endogenous *GRR1* or conditional *GAL1* promoter. In the strains with endogenous *GRR1* promoter, β-estradiol induced transcription of Clb3Δ130. In the strains with *GRR1* under inducible *GAL1* promoter, both Grr1 and Clb3Δ130 expression can be induced with galactose and β-estradiol, respectively. The error bars indicate ± standard error of the mean (s.e.m., single-cell fluorescence data set).

3.2.3 Cks1 module is essential for rapid protein degradation

Cks1 priming enhances the affinity of the Cdc28-cyclin complex to the downstream-located phosphosites and, hence, can increase phosphorylation rates but is not essential for consensus motif phosphorylation. Thus, we decided to test how the Cks1 priming module would influence the degradation rates of the tagged proteins. The Cks1 priming is distance-dependent with an optimal distance between phosphosites 12-16 aa. The distance between Cks1 priming T5 and downstream T33 is 27 aa (Figure 6A). Shortening the distance, likely, could improve the multisite phosphorylation rates and, hence, speed up protein degradation.

Previous data showed that mutating T2 and T5 in Sic1 leads to decreased multisite phosphorylation rates (Kõivomägi et al., 2011a). We wanted to analyse the effect of those phosphosites in the context of our synthetic degron tag.

To do that, we tested three tag variants with a modified Cks1 module: 1) with the shortened distance between T5 and T33 (Figure 6A, TT(-9)T STST 2×PxF Sic1C); 2) with truncated T2 and T5 (Figure 6A, T STST 2×PxF Sic1C); 3) and with the whole Cks1-priming module removed (Figure 6A, STST 2×PxF Sic1C). In the case of shortening the T5-T33 distance, we expected to see an increase in degradation rates due to enhanced multisite phosphorylation, as 18 aa is closer to optimal distance than the initial 27 aa. Surprisingly, the results show that degradation rates of FL tag and variant with shortened T5-T33 distance did not differ. However, both deletion and truncation of the Cks1 module caused almost doubling of protein half-life (from around 25 min for FL to nearly 50 min for truncated variants, Figure 6B). The mCherry fluorescence in the strain completely lacking priming module was more stable than in the one with T33 site (Figure 6B). These results suggest that both the distance and the overall context might play a role in Cks1-dependent multisite phosphorylation (supported by the results in 3.2.4). However, further experiments are required to prove or discard this hypothesis.

3.2.4 Deletion of 9 amino acids between T57 and S79 caused mCherry stabilization

Cln2 degron is less studied than Sic1, but we hypothesized that threonine phosphosite located close to the priming module, T57, could primes phosphorylation of the downstream diphosphodegron S79 and T82 (similar to the situation when T45/T48 primes phosphorylation of S69, S76, and S80 in Sic1 (Figure 1)). Therefore, shortening the distance between T57 and S79 was expected to increase the multisite phosphorylation rate. We tested two

variants: TTT ST(-3)ST 2×PxF Sic1C, where T57-S79 distance was shortened to 18 aa, and TTT ST(-9)ST 2×PxF Sic1C with 12 aa distance (Figure 6A). For the 18 aa variant, the results show a slight delay in degradation compared to the FL tag; however, the 12 aa variant almost fully stabilized the protein (Figure 6C). These results contradict the data on the distance between phosphosites optimal for Cks1 priming. A possible explanation can be an impairment of Grr1 recognition of the shortened phosphodegron tag caused either by shortening itself or deletion of some unknown motifs, essential for the binding. Further research is required.

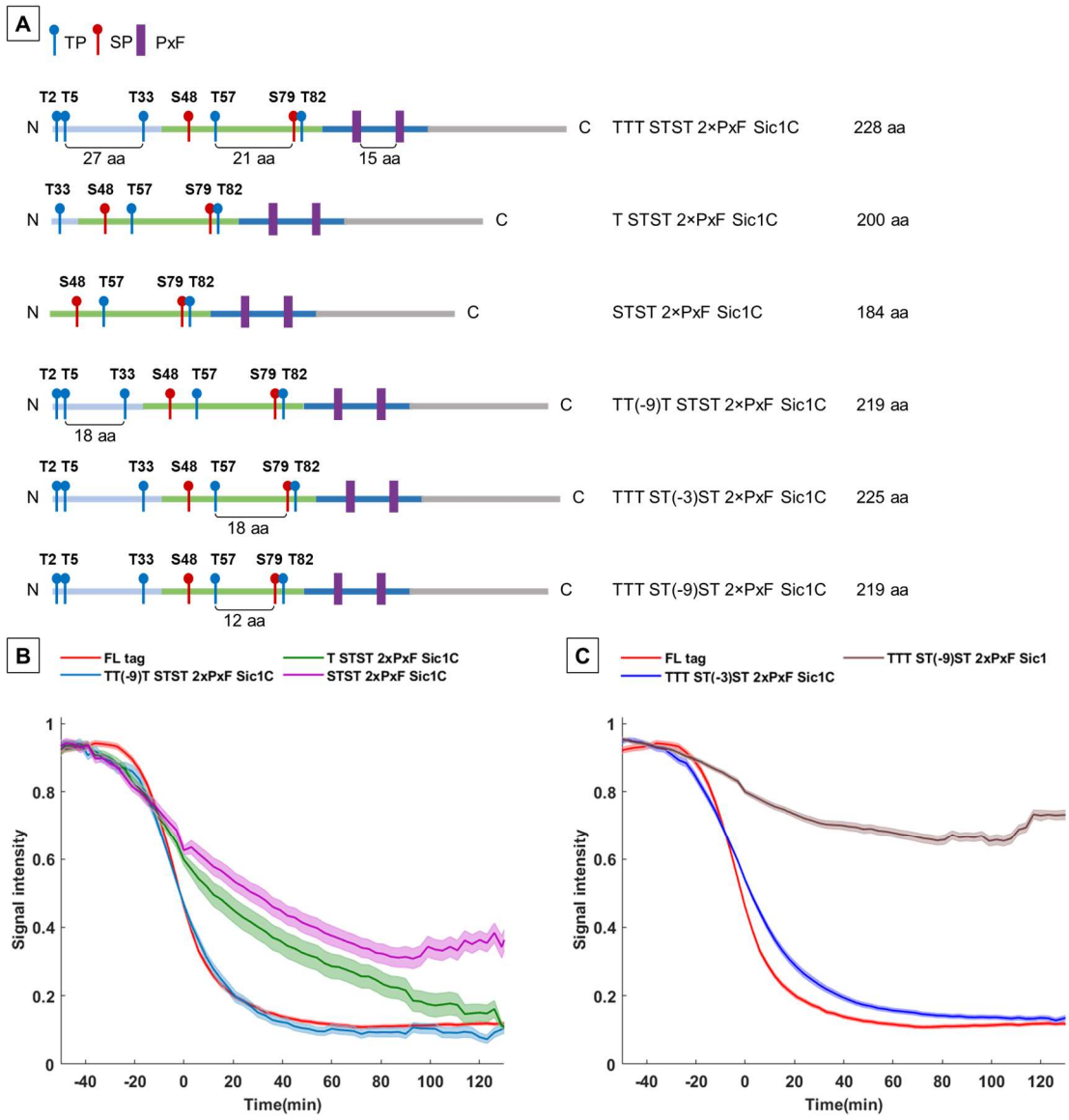

Figure 6. A, Schematic representations of phosphodegron tags used in **B** and **C**. **B**, Plot showing synchronized, normalized to maximum, mean cytoplasmic levels of mCherry tagged with variants with shortened Cks1 module. **C**, Plot showing synchronized, normal-

ized to maximum, mean cytoplasmic levels of mCherry tagged with variants with a shortened distance between T57 and S79. For both **B** and **C**, the error bars are ± standard error mean (s.e.m.) from the single-cell fluorescence sample set.

3.2.5 Presence of the second PxF in the tag and its location in relation to phosphodegron module are not crucial

Researchers found that the location of the docking motif with respect to phosphosites might influence phosphorylation rates (Kõivomägi et al., 2011a). PxF is a recently discovered Clb3 docking motif. In the Ypr174c protein, where this motif was mapped, 20-35 aa separates docking motif and phosphosites (Örd et al., 2020). In FL phosphodegron tag, the distance between the first PxF and S48-T57 phosphosites and the distance between the second PxF and S79-T82 is around 60 aa in both cases. Shortening the distance between PxF sites would bring the second PxF closer to S79-T82, which might enhance phosphorylation rates and further contribute to tag optimization. As there is more to investigate concerning PxF docking, we decided to test variants with a single PxF motif (Figure 7A, TTT STST PxF GSA and TTT STST PxF). Variant with no linker after the single PxF showed very good degradation rates (Figure 7B), but the absolute level of mCherry fluorescence was initially almost twice lower than in the strain with FL-tagged mCherry (Figure 7C). It could result from conformational changes in mCherry protein due to the absence of the flexible linker between phosphodegron tag and reporter protein (additional results and further discussion can be found in section 3.2.6).

Shortening the sequence between two Clb3 docking sites did not reduce the degradation rates and even brought mCherry fluorescence to slightly lower levels when compared to the FL tag (Figure 7D). Variant with only one PxF docking motif and GSA linker instead of Sic1C displayed moderate decrease of degradation rates and elevated mCherry levels. For further understanding, variants with 1) single PxF and Sic1C linker, and 2) 2×PxF and GSA linker have to be tested. Based on the results obtained, we can suggest that the effect of one PxF deletion is not too pronounced.

3.2.6 Sic1C linker truncation stabilizes the protein; TTT STST PxF tag causes severe decrease in protein abundance prior to induction

Sic1C linker module was initially present in the FL phosphodegron tag to introduce space between tagged protein and functional elements of the phosphodegron tag if we talk about 3D protein structure. It can be required both for proper protein function and free access of

the Cdc28-cyclin-Cks1 complex to the tag. However, Sic1C is relatively long (96 aa) and may contain some unknown regulatory sequences. Thus, we designed variants with Sic1C exchanged for flexible GSA linker, no linkers at all, and Sic1CΔ74 (120-141 aa of Sic1C) (Figure 7A, TTT STST PxF GSA, TTT STST PxF, TTT STST 2×PxF, and TTT STST 2×PxF Sic1CΔ74, respectively). The results show that the truncation of Sic1C linker led to stabilization of mCherry, similar to the situation when no linker was used. In fact, those two variants show very similar behaviour (Figure 7A). Construct with GSA linker was less stable. From that, we could suggest that truncated Sic1C is either less flexible than the full-length Sic1C or does not include sequence elements that compensate for lack of flexibility.

To our surprise, a variant with no Sic1C linker and two PxF docking sites was more stable than a similar variant with a single PxF. As described in 3.2.5, we found that initial mCherry fluorescence levels were much lower for this short variant. To investigate whether the tag affects fluorescence through affecting mCherry conformation or protein degrades more efficiently in the latter case, we performed Western blotting (Figure 8A). The results indicate that mCherry tagging with TTT STST PxF led to decreased initial levels of this protein. We suggest that this could be due to phosphorylation of this tag prior to induction or due to impairment of protein expression at some level. We also performed Western blotting of the parental strain for all further strains carrying tag variants (the strain with untagged mCherry). mCherry there is, as expected, stable, and initial, pre-induction levels of it in FL-tagged strain is comparable with initial levels in strain with untagged mCherry.

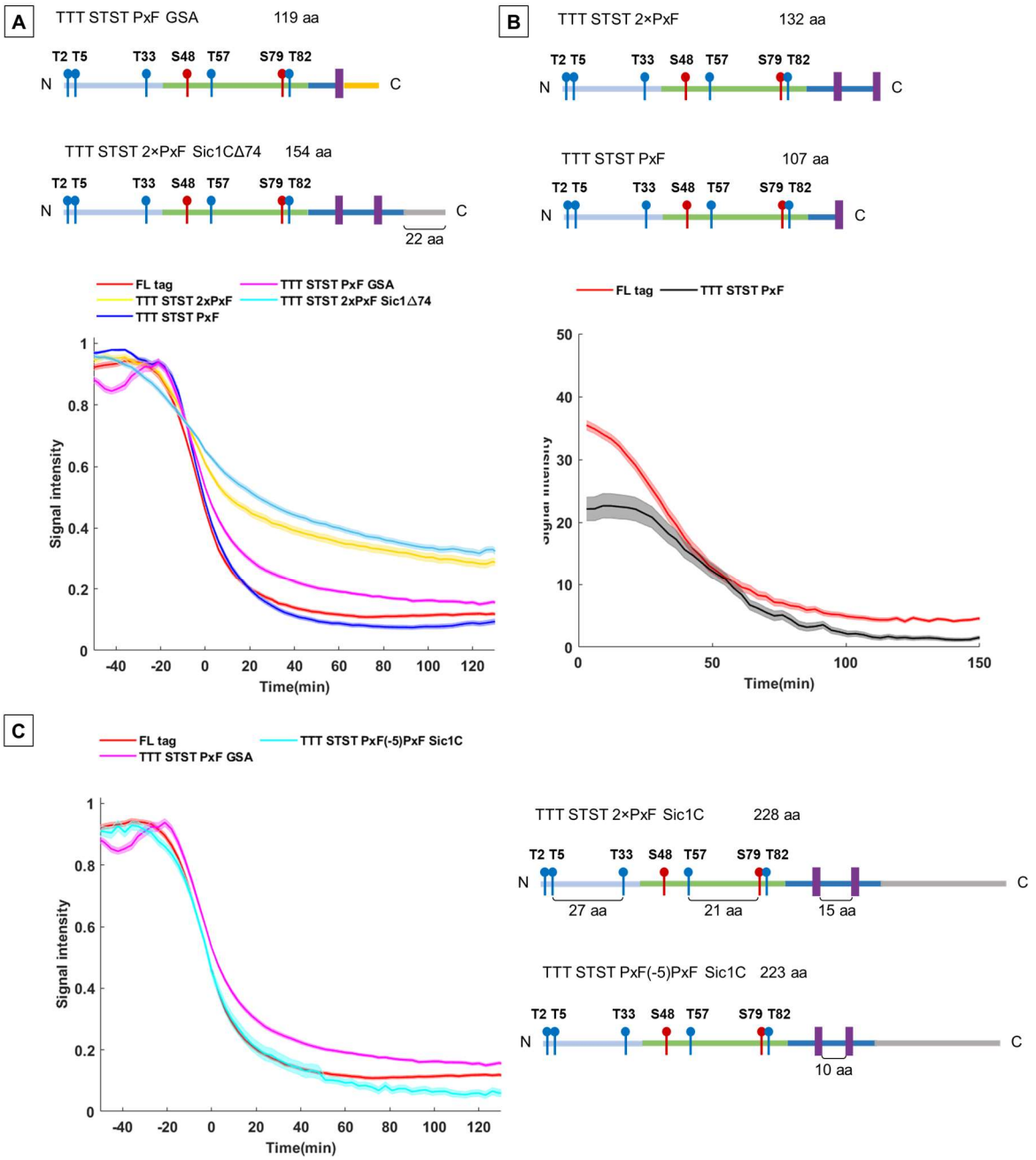

Figure 7. A, Schematic representations of phosphodegron tags used in **B**, **C**, **D**. **B**, Plot showing synchronized, normalized to maximum, mean cytoplasmic levels of mCherry tagged with variants with truncated, deleted or exchanged to GSA linker Sic1C. **C,** Plot showing mean cytoplasmic levels of FL-tagged mCherry and mCherry tagged with deleted Sic1C and second PxF docking site. **D**, Plot showing normalized to maximum, mean cytoplasmic levels of mCherry tagged with a variant with a shortened distance between two PxF motifs and variant with one PxF removed and Sic1C substituted to GSA linker. For **B**, **C**, and **D** the error bars are ± standard error mean (s.e.m.) from the single-cell fluorescence sample set.

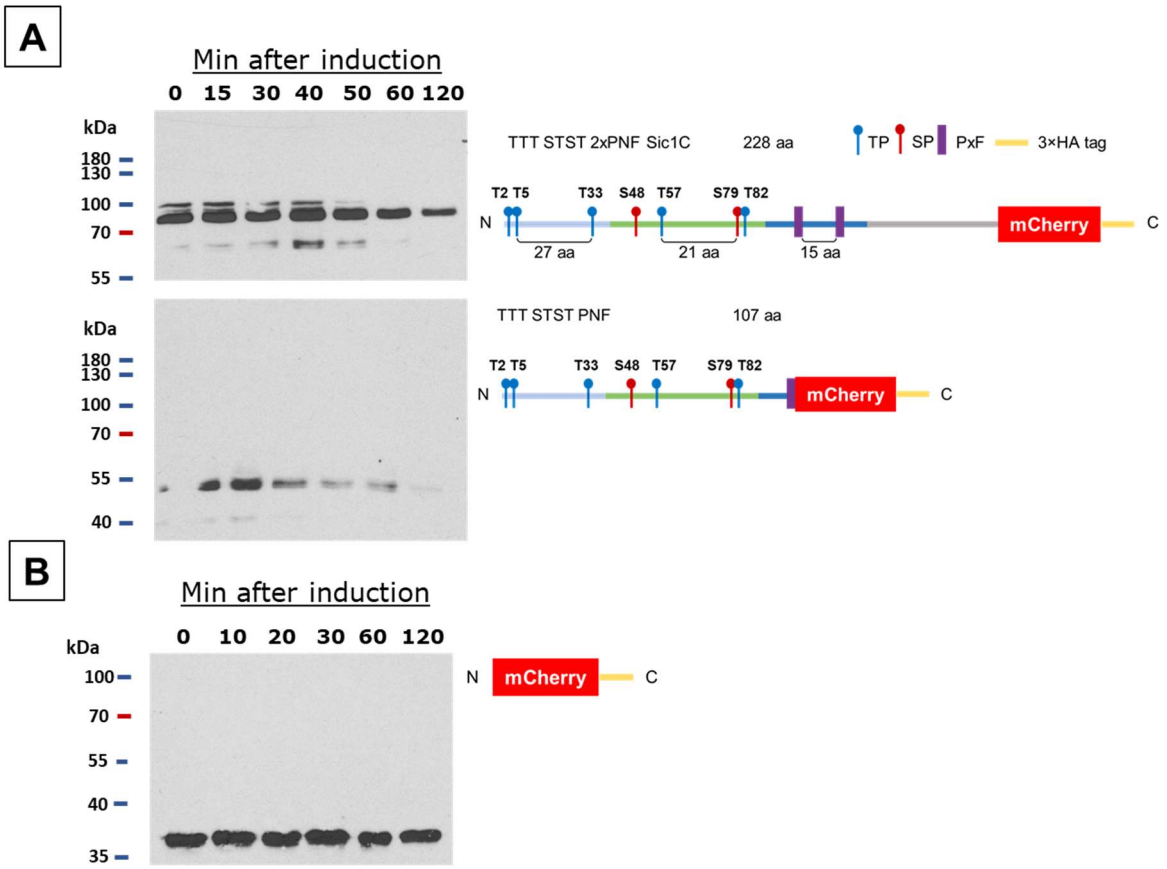

Figure 8. Western blotting for mCherry levels estimation. **A**, Levels of FL-tagged mCherry and mCherry tagged with short phosphodegron tag without Sic1C linker and with one docking site removed. The first timepoint (0) was taken prior to induction and demonstrated level of mCherry in non-induced culture. Due to the transfer problem, first timepoint for shorter tag is absent. **B**, Levels on untagged mCherry in induced (Grr1 and Clb3Δ130) culture.

SUMMARY

In this study, we successfully reproduced the system for inducible protein degradation previously developed in our lab, in a new strain. The system was shown to be replicable, and protein tagging with phosphodegron tags results in the same degradation profiles in different strains. In addition, we established a workflow for protein tagging utilizing CRISPR/Cas9 system, which allows to tag proteins without genomic integration of the selection marker.

By comparing strains with endogenous and conditional Grr1 F-box protein expression, we discovered that in the absence of Clb3-Cdc28 complex in the cell, phosphodegron tag is phosphorylated by other cyclin-Cdc28 complexes regardless of docking motifs.

From the set of shortened tags we designed, three show approximately the same degradation rates as full-length degron: TT(-9)T STST 2×PxF Sic1C, TTT ST(-3)ST 2×PxF Sic1, and TTT STST PxF(-5)PxF Sic1C. The next step in the design of the shortest optimal tag could be the combination of those variants in a single degron TT(-9)T ST(-3)ST PxF(-5)PxF Sic1C.

A variety of phosphodegron tags with different output degradation rates developed in this study will allow to conditionally downregulate the protein of interest. However, the efficacy of this method also depends on the native expression levels of the protein. Proteins under weaker promoters likely will be regulated more efficiently by degradation. Another aspect to consider is the coupling of transcriptional and translational regulation. If tight control and complete elimination of protein from the cell is required, there is a need for both switching off the promoter and degrading the protein.

However, to prove that our targeted degradation system can be used in industry, further experiments are needed. The first step would be tagging of metabolic enzymes to prove that tag addition does not influence enzymatic activity prior the induction. The cell density of the cultures in industrial bioreactors is high, and gradual upscaling and optimization is needed to adapt the system for industrial purposes.

REFERENCES

Bailly, E., Cabantous, S., Sondaz, D., Bernadac, A., and Simon, M.N. (2003). Differential cellular localization among mitotic cyclins from Saccharomyces cerevisiae: A new role for the axial budding protein Bud3 in targeting Clb2 to the mother-bud neck. J. Cell Sci. *116*, 4119–4130.

Berset, C., Griac, P., Tempel, R., La Rue, J., Wittenberg, C., and Lanker, S. (2002). Transferable Domain in the G1 Cyclin Cln2 Sufficient To Switch Degradation of Sic1 from the E3 Ubiquitin Ligase SCFCdc4 to SCFGrr1. Mol. Cell. Biol. *22*, 4463–4476.

Bhaduri, S., and Pryciak, P.M. (2011). Cyclin-specific docking motifs promote phosphorylation of yeast signaling proteins by G1/S Cdk complexes. Curr. Biol. *21*, 1615–1623.

Blazeck, J., Garg, R., Reed, B., and Alper, H.S. (2012). Controlling promoter strength and regulation in Saccharomyces cerevisiae using synthetic hybrid promoters. Biotechnol. Bioeng. *109*, 2884–2895.

De Bondt, H.L., Rosenblatt, J., Jancarik, J., Jones, H.D., Morgant, D.O., and Kim, S.H. (1993). Crystal structure of cyclin-dependent kinase 2. Nature.

Bononi, A., Agnoletto, C., De Marchi, E., Marchi, S., Patergnani, S., Bonora, M., Giorgi, C., Missiroli, S., Poletti, F., Rimessi, A., et al. (2011). Protein kinases and phosphatases in the control of cell fate. Enzyme Res. *2011*.

Contegno, F., Cioce, M., Pelicci, P.G., and Minucci, S. (2002). Targeting protein inactivation through an oligomerization chain reaction. Proc. Natl. Acad. Sci. U. S. A. *99*, 1865–1869.

Cross, F.R., and Yuste-Rojas, M. (1999). Specialization and Targeting of B-Type Cyclins to the prereplicative complex (PRC) (Tanaka et al the possibility of divergent function to ask whether the.

Doncic, A., Eser, U., Atay, O., and Skotheim, J.M. (2013). An Algorithm to Automate Yeast Segmentation and Tracking. PLoS One.

Elbashir, S.M., Harborth, J., Lendeckel, W., Yalcin, A., Weber, K., and Tuschl, T. (2001). Duplexes of 21-nucleotide RNAs mediate RNA interference in cultured mammalian cells. Nature *411*, 494–498.

Epstein, C.B., and Cross, F.R. (1992). CLB5: A novel B cyclin from budding yeast with a role in S phase. Genes Dev. *6*, 1695–1706.

Faustova, I., Bulatovic, L., Matiyevskaya, F., Valk, E., Örd, M., and Loog, M. (2021). A new linear cyclin docking motif that mediates exclusively S-phase CDK-specific signaling. EMBO J. *40*, e105839.

Feldman, R.M.R., Correll, C.C., Kaplan, K.B., and Deshaies, R.J. (1997). A complex of Cdc4p, Skp1p, and Cdc53p/cullin catalyzes ubiquitination of the phosphorylated CDK inhibitor Sic1p. Cell *91*, 221–230.

Flick, J.S., and Johnston, M. (1991). GRR1 of Saccharomyces cerevisiae is required for glucose repression and encodes a protein with leucine-rich repeats. Mol. Cell. Biol. *11*, 5101–5112.

Gnügge, R., Liphardt, T., and Rudolf, F. (2016). A shuttle vector series for precise genetic engineering of Saccharomyces cerevisiae. Yeast *33*, 83–98.

Gordley, R.M., Williams, R.E., Bashor, C.J., Toettcher, J.E., Yan, S., and Lim, W.A. (2016). Engineering dynamical control of cell fate switching using synthetic phospho-regulons. Proc. Natl. Acad. Sci. U. S. A. *113*, 13528–13533.

Hao, B., Oehlmann, S., Sowa, M.E., Harper, J.W., and Pavletich, N.P. (2007). Structure of a Fbw7-Skp1-Cyclin E Complex: Multisite-Phosphorylated Substrate Recognition by SCF Ubiquitin Ligases. Mol. Cell *26*, 131–143.

Hegemann, J.H., and Heick, S.B. (2011). Delete and repeat: A comprehensive toolkit for sequential gene knockout in the budding yeast saccharomyces cerevisiae. Methods Mol. Biol. *765*, 189–206.

Ho, B., Baryshnikova, A., and Brown, G.W. (2018). Unification of Protein Abundance Datasets Yields a Quantitative Saccharomyces cerevisiae Proteome. Cell Syst.

Hodge, A., and Mendenhall, M. (1999). The cyclin-dependent kinase inhibitory domain of the yeast Sic1 protein is contained within the C-terminal 70 amino acids. Mol. Gen. Genet. *262*, 55–64.

Holt, L.J. (2012). Regulatory modules: Coupling protein stability to phopshoregulation during cell division. FEBS Lett.

Holt, L.J., Tuch, B.B., Villen, J., Johnson, A.D., Gygi, S.P., and Morgan, D.O. (2009). Global analysis of cdk1 substrate phosphorylation sites provides insiqhts into evolution. Science (80-.). *325*, 1682–1686.

Jakubowski, H. V., and Spinali, K. (2017). Cell signaling: Principles and mechanisms.

Biochem. Mol. Biol. Educ. *45*, 365–367.

Jensen, E.D., Ferreira, R., Jakočiunas, T., Arsovska, D., Zhang, J., Ding, L., Smith, J.D., David, F., Nielsen, J., Jensen, M.K., et al. (2017). Transcriptional reprogramming in yeast using dCas9 and combinatorial gRNA strategies. Microb. Cell Fact. *16*, 46.

Jordan, J.D., Landau, E.M., and Iyengar, R. (2000). Signaling networks: The origins of cellular multitasking. Cell *103*, 193–200.

Kõivomägi, M., Valk, E., Venta, R., Iofik, A., Lepiku, M., Balog, E.R.M., Rubin, S.M., Morgan, D.O., and Loog, M. (2011a). Cascades of multisite phosphorylation control Sic1 destruction at the onset of S phase. Nature *480*, 128–131.

Kõivomägi, M., Valk, E., Venta, R., Iofik, A., Lepiku, M., Morgan, D.O., and Loog, M. (2011b). Dynamics of Cdk1 Substrate Specificity during the Cell Cycle. Mol. Cell *42*, 610–623.

Kõivomägi, M., Örd, M., Iofik, A., Valk, E., Venta, R., Faustova, I., Kivi, R., Balog, E.R.M., Rubin, S.M., and Loog, M. (2013). Multisite phosphorylation networks as signal processors for Cdk1. Nat. Struct. Mol. Biol. *20*, 1415–1424.

Landry, B.D., Doyle, J.P., Toczyski, D.P., and Benanti, J.A. (2012). F-box protein specificity for G1 cyclins is dictated by subcellular localization. PLoS Genet. *8*.

Loog, M., and Morgan, D.O. (2005a). Cyclin specificity in the phosphorylation of cyclin-dependent kinase substrates. Nature *434*, 104–108.

Loog, M., and Morgan, D.O. (2005b). Cyclin specificity in the phosphorylation of cyclin-dependent kinase substrates. Nature *434*, 104–108.

Mateus, C., and Avery, S. V. (2000). Destabilized green fluorescent protein for monitoring dynamic changes in yeast gene expression with flow cytometry. Yeast.

McCusker, D., Denison, C., Anderson, S., Egelhofer, T.A., Yates, J.R., Gygi, S.P., and Kellogg, D.R. (2007). Cdk1 coordinates cell-surface growth with the cell cycle. Nat. Cell Biol. *9*, 506–515.

McGrath, D.A., Balog, E.R.M., Kõivomägi, M., Lucena, R., Mai, M. V., Hirschi, A., Kellogg, D.R., Loog, M., and Rubin, S.M. (2013). Cks confers specificity to phosphorylation-dependent CDK signaling pathways. Nat. Struct. Mol. Biol.

Morgan, D.O. (2007). The Cell Cycle: Principles of Control (London: New Science Press Ltd).

Niopek, D., Benzinger, D., Roensch, J., Draebing, T., Wehler, P., Eils, R., and Di Ventura, B. (2014). Engineering light-inducible nuclear localization signals for precise spatiotemporal control of protein dynamics in living cells. Nat. Commun. *5*, 1–11.

Nishimura, K., Fukagawa, T., Takisawa, H., Kakimoto, T., and Kanemaki, M. (2009). An auxin-based degron system for the rapid depletion of proteins in nonplant cells. Nat. Methods *6*, 917–922.

Norrander, J., Kempe, T., and Messing, J. (1983). Construction of improved M13 vectors using oligodeoxynucleotide-directed mutagenesis. Gene *26*, 101–106.

Örd, M., and Loog, M. (2019). How the cell cycle clock ticks. Mol. Biol. Cell *30*, 169–172.

Örd, M., Venta, R., Möll, K., Valk, E., and Loog, M. (2019a). Cyclin-Specific Docking Mechanisms Reveal the Complexity of M-CDK Function in the Cell Cycle. Mol. Cell *75*, 76-89.e3.

Örd, M., Möll, K., Agerova, A., Kivi, R., Faustova, I., Venta, R., Valk, E., and Loog, M. (2019b). Multisite phosphorylation code of CDK. Nat. Struct. Mol. Biol. *26*, 649–658.

Örd, M., Puss, K.K., Kivi, R., Möll, K., Ojala, T., Borovko, I., Faustova, I., Venta, R., Valk, E., Kõivomägi, M., et al. (2020). Proline-Rich Motifs Control G2-CDK Target Phosphorylation and Priming an Anchoring Protein for Polo Kinase Localization. Cell Rep. *31*, 107757.

Ottoz, D.S.M., Rudolf, F., and Stelling, J. (2014). Inducible, tightly regulated and growth condition-independent transcription factor in Saccharomyces cerevisiae. Nucleic Acids Res. *42*.

Pecani, K., and Cross, F.R. (2016). Degradation of the Mitotic Cyclin Clb3 Is not Required for Mitotic Exit but Is Necessary for G1 Cyclin Control of the Succeeding Cell Cycle. Genetics *204*, 1479–1494.

Russo, A.A., Jeffrey, P.D., and Pavletich, N.P. (1996). Structural basis of cyclin-dependent kinase activation by phosphorylation. Nat. Struct. Biol.

Shaw, W. Quick and easy CRISPR engineering in Saccharomyces cerevisiae · Benchling.

Skowyra, D., Craig, K.L., Tyers, M., Elledge, S.J., and Harper, J.W. (1997). F-box proteins are receptors that recruit phosphorylated substrates to the SCF ubiquitin-ligase complex. Cell *91*, 209–219.

Smith, G.K., Ke, Z., Guo, H., and Hengge, A.C. (2011). Insights into the Phosphoryl

Transfer Mechanism of Cyclindependent Protein Kinases from Ab Initio QM/MM Free-energy Studies. J Phys Chem B. *115*, 13713–13722.

Tyanova, S., Cox, J., Olsen, J., Mann, M., and Frishman, D. (2013). Phosphorylation Variation during the Cell Cycle Scales with Structural Propensities of Proteins. PLoS Comput. Biol. *9*, 1002842.

Venta, R., Valk, E., Örd, M., Košik, O., Pääbo, K., Maljavin, A., Kivi, R., Faustova, I., Shtaida, N., Lepiku, M., et al. (2020). A processive phosphorylation circuit with multiple kinase inputs and mutually diversional routes controls G1/S decision. Nat. Commun. *11*, 1–14.

Wu, T., Yoon, H., Xiong, Y., Dixon-Clarke, S.E., Nowak, R.P., and Fischer, E.S. (2020). Targeted protein degradation as a powerful research tool in basic biology and drug target discovery. Nat. Struct. Mol. Biol. *27*, 605–614.

Appendix

Supplementary information

Supplementary Table 1. Extended list of strains, used in this study, including genotypes.

Strain	Genotype*	Short description	Source/ Reference
RKI450 RKI451 RKI452	*his3::pACT1-LexA-ER-B112::HIS3* *ura3::pEstr-Clb3Δ130-NES-EGFP::URA3* *CLB3::TRP1* *leu2::pADH1-Degron(TTT STST 2×PxF Sic1C)-mCherry-3HA*	LexA-ER-B112 transcription factor coding sequence under the constitutive *ACT1* promoter, kinase input (truncated Clb3 fused to NES and EGFP, more information in Results section) coding sequence under the synthetic inducible pEstr promoter, deletion of the endogenous *CLB3* gene.	Our lab, Rait Kivi Transcription factor cassette was integrated using FRP880 plasmid, which was a gift from Joerg Stelling (Ottoz et al., 2014)
RKI453	*his3::pACT1-LexA-ER-B112::HIS3* *ura3::pEstr-Clb3Δ130-NES-EGFP::URA3* *CLB3::TRP1* *leu2::pADH1-Degron(TTT AAAA 2×PxF Sic1C)-mCherry-3HA*	Same as RKI450-452, but STST phosphosites are mutated to alanine amino acids	
RKI456	*his3::pACT1-LexA-ER-B112::HIS3* *ura3::pEstr-Clb3Δ130-NES-EGFP::URA3* *CLB3::TRP1*	Same as RKI450-452, but no mCherry integration	
RKI514	*his3::pACT1-LexA-ER-B112::HIS3* *ura3::pEstr-Clb3Δ130-NES-EGFP::URA3* *CLB3::TRP1*	Parental strain: RKI456 Replacement of the endogenous *GRR1* promoter with the inducible *GAL1*	

Strain	Genotype*	Short description	Source/ Reference
	GRR1::pGAL1-3HA-GRR1:NatNT	promoter for the regulation of *GRR1* transcription	
RKI521	*his3::pACT1-LexA-ERB112::HIS3* *ura3::pEstr-Clb3Δ130-NESEGFP::URA3* *CLB3::TRP1* *GRR1::pGAL1-3HA-GRR1:NatNT* *leu2::pADH1-Degron(TTT AAAA 2×PxF Sic1C)-mCherry-3HA*	Parental strain: RKI453 Replacement of the endogenous *GRR1* promoter with the inducible *GAL1* promoter for the regulation of *GRR1* transcription	
NS352	*his3::pACT1-LexA-ERB112::HIS3* *ura3::pEstr-Clb3Δ130-NESEGFP::URA3* *CLB3::TRP1* *GRR1::pGAL1-3HA-GRR1:NatNT* *leu2::pRG205mx-pADH1-NES-mCherry-3HA-tCyc1::LEU2*	Parental strain: RKI514; Integration of an output (reporter) module: mCherry fused with NES from the N-terminus and 3xHA tag from the C-terminus under the *Adh1* promoter	This study
NS354 NS355	*his3::pACT1-LexA-ERB112::HIS3* *ura3::pEstr-Clb3Δ130-NESEGFP::URA3* *CLB3::TRP1* *GRR1::pGAL1-3HA-GRR1:NatNT* *leu2::pADH1-Degron(TTT STST 2×PxF Sic1C)-mCherry-3HA*	Parental strain: NS352; mCherry tagged with TTT STST 2×PxF Sic1C degron tag from N-term	

Strain	Genotype*	Short description	Source/ Reference
NS358 NS359	*his3::pACT1-LexA-ER-B112::HIS3* *ura3::pEstr-Clb3Δ130-NES-EGFP::URA3* *CLB3::TRP1* *GRR1::pGAL1-3HA-GRR1:NatNT* *leu2::pADH1-Degron(TTT STST 2×PxF)-mCherry-3HA*	Parental strain: NS352; mCherry tagged with TTT STST 2×PxF degron tag from N-term	
NS360 NS361 NS362	*his3::pACT1-LexA-ER-B112::HIS3* *ura3::pEstr-Clb3Δ130-NES-EGFP::URA3* *CLB3::TRP1* *GRR1::pEstr-3HA-GRR1:NatNT* *leu2::pADH1-Degron(TTT STST 2×PxF Sic1C)-mCherry-3HA*	Parental strain: NS354; Replacement of inducible *GAL1* promoter with the inducible promoter pEstr for the regulation of *GRR1* transcription	
NS364 NS365	*his3::pACT1-LexA-ER-B112::HIS3* *ura3::pEstr-Clb3Δ130-NES-EGFP::URA3* *CLB3::TRP1* *GRR1::pGAL1-3HA-GRR1:NatNT* *leu2::pADH1-Degron(TTT ST(-3)ST 2×PxF Sic1C)-mCherry-3HA*	Parental strain: NS352; mCherry tagged with TTT ST(-3)ST 2×PxF Sic1C degron tag from N-term	
NS366 NS367	*his3::pACT1-LexA-ER-B112::HIS3* *ura3::pEstr-Clb3Δ130-NES-EGFP::URA3*	Parental strain: NS352; mCherry tagged with TTT ST(-9)ST 2×PxF Sic1C degron tag from N-term	

Strain	Genotype*	Short description	Source/ Reference
	CLB3::TRP1 *GRR1::pGAL1-3HA-GRR1:NatNT* *leu2::pADH1-Degron(TTTST(-9)ST 2×PxF Sic1C)-mCherry-3HA*		
NS368 NS369	*his3::pACT1-LexA-ER-B112::HIS3* *ura3::pEstr-Clb3Δ130-NES-EGFP::URA3* *CLB3::TRP1* *GRR1::pGAL1-3HA-GRR1:NatNT* *leu2::pADH1-Degron(TT(-9)TSTST 2×PxF Sic1C)-mCherry-3HA*	Parental strain: NS352; mCherry tagged with TT(-9)T STST 2×PxF Sic1C degron tag from N-term	
NS370 NS371	*his3::pACT1-LexA-ER-B112::HIS3* *ura3::pEstr-Clb3Δ130-NES-EGFP::URA3* *CLB3::TRP1* *GRR1::pGAL1-3HA-GRR1:NatNT* *leu2::pADH1-Degron(TTTSTST PxF(-5)PxF Sic1C)-mCherry-3HA*	Parental strain: NS352; mCherry tagged with TTT STST PxF(-5)PxF Sic1C degron tag from N-term	
NS372 NS373	*his3::pACT1-LexA-ER-B112::HIS3* *ura3::pEstr-Clb3Δ130-NES-EGFP::URA3* *CLB3::TRP1* *GRR1::pGAL1-3HA-GRR1:NatNT*	Parental strain: NS352; mCherry tagged with TTT STST PxF degron tag from N-term	

Strain	Genotype*	Short description	Source/ Reference
	leu2::pADH1-Degron(TTT STST PxF)-mCherry-3HA		
NS374 NS375	*his3::pACT1-LexA-ER-B112::HIS3* *ura3::pEstr-Clb3Δ130-NES-EGFP::URA3* *CLB3::TRP1* *GRR1::pGAL1-3HA-GRR1:NatNT* *leu2::pADH1-Degron(TTT STST PxF GSA linker)-mCherry-3HA*	Parental strain: NS352; mCherry tagged with TTT STST PxF GSA linker degron tag from N-term	
NS376 NS377	*his3::pACT1-LexA-ER-B112::HIS3* *ura3::pEstr-Clb3Δ130-NES-EGFP::URA3* *CLB3::TRP1* *GRR1::pGAL1-3HA-GRR1:NatNT* *leu2::pADH1-Degron(T STST 2×PxF Sic1C)-mCherry-3HA*	Parental strain: NS352; mCherry tagged with T STST 2×PxF Sic1C degron tag from N-term	
NS378 NS379	*his3::pACT1-LexA-ER-B112::HIS3* *ura3::pEstr-Clb3Δ130-NES-EGFP::URA3* *CLB3::TRP1* *GRR1::pGAL1-3HA-GRR1:NatNT* *leu2::pADH1-Degron(STST 2×PxF Sic1C)-mCherry-3HA*	Parental strain: NS352; mCherry tagged with STST 2×PxF Sic1C degron tag from N-term	
NS391 NS392 NS393	*his3::pACT1-LexA-ER-B112::HIS3*	Parental strain: NS352;	

Strain	Genotype*	Short description	Source/ Reference
	ura3::pEstr-Clb3Δ130-NES-EGFP::URA3 *CLB3::TRP1* *GRR1::pGAL1-3HA-GRR1:NatNT* *leu2::pADH1-Degron(TTT STST 2×PxF Sic1C23aa)-mCherry-3HA*	mCherry tagged with TTT STST 2×PxF Sic1C23aa degron tag from N-term	

* Yeast strains are MATa haploids of the W303 strain. All strains created in this work are based on RKI514 and common genetic background is not described. Strains, constructed in this study, were generated with lithium acetate mediated transformation (see Methods).

Supplementary Table 2. Primers used in this study.

Number in the lab database	Sequence
2316	CCT TGG AGC CGT ACA TGA ACT GAG
6173	CCT TTC TTC CTT GTT TCT TTT TC
6175	CCC TCG ATC TCG AAC TCG
6378	ACG CGC CGA AGG CCG CCA CTC CAC CGG CG
6379	TCG TAC TGT TCT ACG ATG GTG TAG TCC TCG TTG TGG G
6388	TGG CGG TCT GGG TGC CCT CGT AGG GGC GGC CCT CGC CCT CGC CCT CGA TCT CGA ACT CG
6389	TTA ATC TTT TGT TTC CTC GTC ATT GTT CTC GTT CCC TTT CTT CCT TGT TTC TTT TTC
6499	AGA GAG TGA GCT CAT GTT TCT CAT TGG
6500	GTT TTC AGC CGG AAT ATG GAA CAA TC
6501	TGA GCT CAT GTT TCT CAT TGG AG
6502	TTC AGC CGG AAT ATG GAA CAA TCA TC
6503	GCT CAT GTT TCT CAT TGG AGT GTG
6504	AGC CGG AAT ATG GAA CAA TCA TCA C
6505	CTT GGC GTA GAA ATT AGG ACC C
6506	AGC GGA GCC AGC GGA TCC CTT GGC GTA GAA ATT AGG ACC CTT TGG
6507	GTT GTC GTG GGA CTC CTT GGC G
6508	GAG CAA GAA CCT TTA CCC CCA AAG
6509	CTT GGC GTA GAA GTT GGG GC
6510	AGC GGA GCC AGC GGA TCC CTT GGC GTA GAA GTT GGG GC
6511	GTA TCT GGT TCC ACG AGA CCT TG
6512	AGT TCT GCT TTA ATG CAG GGA C
6534	GCT GGT TCT GGC GAA TTC ATG GTG AGC AAA GGC GAG G
6535	ATG GTG AGC AAA GGC GAG G
6684	TTT ATT GAT GTC CAA GCC TGC CAG C
6685	ATG CAG GGA CAA AAG ACC CCA CAG AAG

6686	TCC ATT CCT TCG CCC GCT TC
6804	ATG GTG AGC AAA GGC GAG GAA GAT AAC
6805	GGA GGC GGC AGC CGC AG

NON-EXCLUSIVE LICENCE TO REPRODUCE THESIS AND MAKE THESIS PUBLIC

I, _Aleksandra Panfilova_,

(*author's name*)

1. herewith grant the University of Tartu a free permit (non-exclusive licence) to

reproduce, for the purpose of preservation, including for adding to the DSpace digital archives until the expiry of the term of copyright,

Optimization of Sic1-Cln2-based phosphodegron tag for inducible protein degradation,

(*title of thesis*)

supervised by _PhD. Nastassia Shtaida and Professor, PhD. Mart Loog_.

(*supervisor's name*)

2. I grant the University of Tartu a permit to make the work specified in p. 1 available to the public via the web environment of the University of Tartu, including via the DSpace digital archives, under the Creative Commons licence CC BY NC ND 3.0, which allows, by giving appropriate credit to the author, to reproduce, distribute the work and communicate it to the public, and prohibits the creation of derivative works and any commercial use of the work from *20/05/2024* until the expiry of the term of copyright.

3. I am aware of the fact that the author retains the rights specified in p. 1 and 2.

4. I certify that granting the non-exclusive licence does not infringe other persons' intellectual property rights or rights arising from the personal data protection legislation.

Aleksandra Panfilova

20/05/2021